Deformation Twinning (Update)☆

D Zhang, L Jiang, B Zheng, JM Schoenung, S Mahajan, and EJ Lavernia, University of California, Davis, CA, USA
IJ Beyerlein, Los Alamos National Laboratory, New Mexico, NM, USA
JM Schoenung and EJ Lavernia, University of California, Irvine, CA, USA

1	**Formation of Deformation Twins**	1
1.1	b.c.c. Metals and Alloys	2
1.2	FCC Metals and Alloys and Related Structures	4
1.3	h.c.p. Materials	7
2	**Influence of Material Variables on Twinning**	10
2.1	Temperature	10
2.2	Strain Rate	11
2.3	Pre-strain	12
2.4	Grain Size and Texture in h.c.p. Materials	12
3	**Accommodation of Deformation Twins and their Role in Crack Nucleation**	14
4	**Advanced Techniques for Studying Deformation Twinning in h.c.p. Materials**	16
4.1	EBSD Research	17
4.2	HRTEM and In-situ TEM studies	20
Acknowledgments		22
References		22

At temperatures below those at which individual atoms move by diffusion, slip and twinning are the major deformation modes that enable a solid to change shape under the action of an applied stress. Experiments have shown that in b.c.c. and h.c.p. metals and alloys twins often form at very low plastic strain level, whilst f.c.c. metals do not generally twin until appreciable plastic deformation by slip has occurred. Immediate twinning is often characterized by very rapid formation of twinned regions, giving rise to large load drops, whereas delayed twinning usually has a rather small effect on the observed stress/strain curves. The former type of twinning is also very sensitive to temperature of deformation and to strain rate. The relative contribution of twinning to the overall strain increases as the temperature is lowered or the strain rate is increased. Deformation by slip alone is frequently observed, but many investigators believe that twinning is accompanied or preceded by slip, even though this slip is difficult to detect.

Twinning is especially important in crystals of lower symmetry, for example, h.c.p. metals and alloys, where the five independent slip systems required to satisfy the von Mises criterion for a general deformation of polycrystals may not be available. In this case, Taylor's 'minimum total shear' hypothesis for specifying the active systems has to be expressed in terms of contributions to the overall deformation from both slip and twinning and is correspondingly more complex.

The classical definition of twinning requires that the twin and parent (or matrix) lattices are related either by a reflection in some plane or by a rotation of 180° about some axis. In crystals of high symmetry, these operations are frequently equivalent. In addition to deformation, twins satisfying this definition may form during nucleation and growth processes such as crystal growth from the vapor or liquid, phase transformation, or recrystallization of the solid. Another type of twinning ('transformation twinning') is found in the product structures of many martensitic transformations.

In principle, deformation twins can form by a homogeneous simple shear of parent lattice, and this implies highly coordinated individual atom displacements, in contrast to the apparently chaotic processes of generation and growth of slip bands during glide deformation. However, some recent theories of twinning require the twin to thicken by the random agglomeration of embryonic twins that have been nucleated within slip bands, within grain boundaries, or on twin boundaries. These theories imply that deformation twins have imperfect structures containing many stacking faults.

The present article is concerned only with deformation twinning and covers the following topics: (i) formation of twins in high-symmetry structures; (ii) influence of material variables on twinning; (iii) accommodation of deformation twins and their role in crack nucleation; and (iv) emerging new techniques for studying deformation twinning. For a comprehensive coverage of deformation twinning, the reader is referred to a review by Christian and Mahajan (1995).

☆*Change History*: July 2015. B. Zheng, S. Mahajan, E.J. Lavernia, I.J. Beryerlein, D. Zhang, L. Jiang, and J. Schoenung completely updated the original article to bring it up-to-date with the latest developments and with more recent references.

1 Formation of Deformation Twins

The formation of deformation twins is divided into nucleation, propagation, and growth stages. Twin nuclei may form under the action of applied stress in a near-perfect region of a crystal (homogeneous nucleation) or, alternatively, may form only when a suitable defect configuration is present (heterogeneous nucleation). To date, theoretical calculations and experimental evidence do not support the concept of homogeneous nucleation of twins (Christian and Mahajan, 1995).

Many models of defect-assisted nucleation involve the dissociation of dislocation configuration into a single- or multilayered stacking fault, which then serves as the twin nucleus. Many of these models are specific to the various crystal structures, but it is useful to recognize their certain common features. The twin nuclei consist of faults that are bounded by partial dislocations of the parent crystal and are referred to as twinning partials. Propagation involves movement of the twin front in the interior of the grain. A twin tip may terminate in the grain, at another twin, or most often, at the grain boundary. Growth normal to the twinning plane may be envisaged as an orderly process in which each layer is added successively to the twin nucleus or as the random accumulation of embryonic twin faults. In the following, we will critique some of the models that have been proposed for common crystal structures and compare experimental observations against the predictions of these models.

1.1 b.c.c. Metals and Alloys

Cottrell and Bilby (1951) considered the continuous growth of a b.c.c. twin from an initial single-layer fault formed from the dissociation of a perfect dislocation in the parent lattice. **Figure 1** shows schematically the conceptual framework of their model. A portion (OB) of perfect dislocation line AOBC, having a Burgers vector $\frac{1}{2}[111]$ and lying in the (112) plane in which it cannot glide, dissociates according to the following reactions with nodes at O and B:

$$\tfrac{1}{2}[111] \rightarrow \tfrac{1}{3}[112] + \tfrac{1}{6}[1\bar{1}1] \qquad [1]$$

The Burgers vector of BDEO is $\frac{1}{6}[11\bar{1}]$ and is thus glissile in the (112) plane. If the length EO happens to be in the screw orientation, it may cross-slip onto the $(\bar{1}21)$ plane, resulting in a fault that is bounded by partials OF and FE. A macroscopic twin is assumed to form by repeated rotation of OF around the dislocation OB that is referred to as a pole dislocation. If the node at O moves toward B as OF rotates, the sweeping twinning dislocation climbs onto consecutive $(\bar{1}21)$ planes, resulting in a macroscopic twin whose thickness is determined by the length of OB.

Sleeswyk (1963) proposed that since an unstressed $\frac{1}{2}\langle 11\bar{1}\rangle$ screw dislocation has three-fold symmetry, it may be regarded as having a three-dimensional core with a $\frac{1}{6}[11\bar{1}]$ partial on each of the intersecting {112} planes. Under stress, however, this configuration will be unstable, and the partials could rearrange to form a three-layer twin on the most highly stressed of the {112} planes. The dislocation reaction governing the nucleation of a three-layer twin can be written as

$$\tfrac{1}{2}[111]\text{screws} \rightarrow 3 \times \tfrac{1}{6}[111] \qquad [2]$$

Sleeswyk assumed that the growth normal to the twinning plane also occurred by spiraling of $\frac{1}{6}[111]$ twinning partials around suitable pole dislocations.

Experimental evidence supporting Sleeswyk's twin nucleation model was obtained by Mahajan (1972a, 1975a) and Mahajan *et al.* (1980). **Figure 2** shows an example of the structure observed in molybdenum–rhenium alloys deformed in tension at 77 K. A

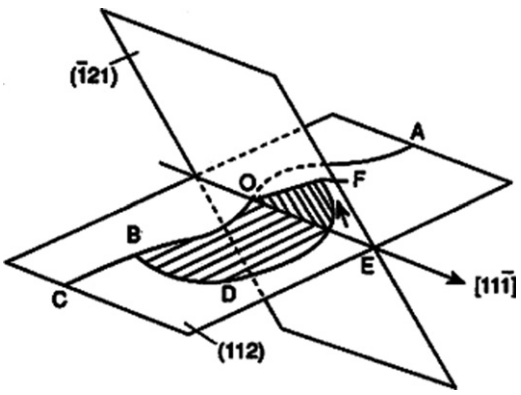

Figure 1 The Cottrell–Bilby pole mechanism for twinning in b.c.c. crystals. AO and BO represent lengths of lattice dislocation of Burgers vector $\frac{1}{2}[111]$, OB is a sessile partial dislocation with Burgers vector $\frac{1}{3}[112]$, referred to as the pole dislocation, and BDEFO is a glissile partial (or twinning) dislocation with Burgers vector $\frac{1}{6}[11\bar{1}]$. There is no dislocation line along OE (after Cottrell and Bilby (1951)).

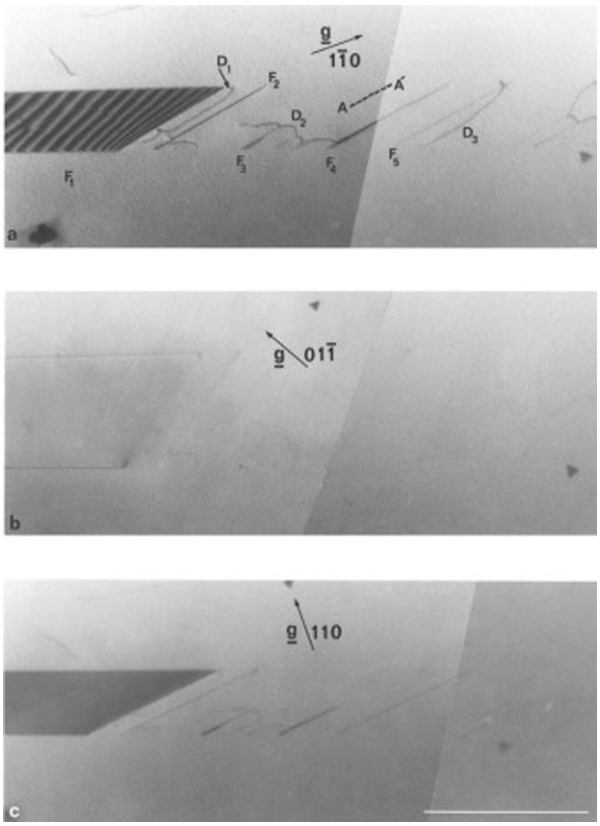

Figure 2 Micrograph showing faults F_1–F_5 and slip dislocations D_1–D_3 in Mo–35 at% Re alloy deformed at 77-K. Results show that F_1–F_5 are twins and that the Burgers vector of D_1–D_3 is parallel to that of twinning partials bounding F_1. AÁ represents the projection of the Burgers vector of D_1–D_3 on the plane of the micrograph (Mahajan, 1972b).

number of faults $F_2 \rightarrow F_5$ and dislocations $D_1 \rightarrow D_3$ are observed ahead of the main fault F_1. Results indicate that F_1 is a twin and is bounded by $\frac{1}{6}[111]$ twinning partials. Furthermore, the observed contrast in **Figure 2(c)**, where the twin is strongly diffracting, suggests that $F_2 \rightarrow F_5$ are also twins that are aligned along the projection of the $[\bar{1}11]$ vector, i.e., AÁ, on the plane of the micrograph in **Figure 2(a)**. It can also be inferred from **Figure 2** that the Burgers vector of twinning partials is parallel to that of slip dislocations, an assessment consistent with the nucleation model of Sleeswyk.

That the above assessment on twin nucleation may be generic in nature is supported by the study of Mahajan *et al.* (1980) on twinning in a spinodally decomposed Fe–Cr–Co alloy, consisting of iron-rich and chromium-rich b.c.c. regions. **Figure 3** shows an interspersion of faults, $F_1 \rightarrow F_8$, and dislocations. The dotted line in **Figure 3(a)** represents the projection of the Burgers vector of slip dislocations onto the plane of the micrograph. The alignment of dislocations with the projection of the Burgers vector suggests that they are screw in character. We can also infer from **Figure 3(b)** that the fault vector associated with $F_1 \rightarrow F_8$ is parallel to the Burgers vector of slip dislocations. Extra spots were observed on electron diffraction patterns and were attributed to twinning.

A dark-field image obtained using one of those spots is shown in **Figure 4**, thus confirming that $F_1 \rightarrow F_8$ are twins. Several interesting observations emerge from **Figure 4**. First, the sides of the twins are aligned along the projection of the twinning vector. Second, twins are not perfect. Third, twins are located at different levels within the foil.

The results of **Figures 2–4** clearly support the view that twins originate from screw-type lattice dislocations. Mahajan (1972a, 1975a) extended the Sleeswyk model by suggesting that the faults formed by the dissociation of screw dislocations thicken by chance encounters with one another as the faults extend in the {112} slip plane. In the original model, the three-layer faults formed by dissociation are bounded on one side by three twinning partials on adjacent {112} planes, and on the other side effectively by two such dislocations and one complementary twinning dislocation to give zero net Burgers vector. When two such faults coalesce, a four-, five-, or six-layer fault may form, depending on the relative displacements of the center plane of the fault. Although this explanation appears to require a high density of dislocations to produce a macroscopic twin, Mahajan suggested that 'slip band conversion' might obviate the need for a pole-type mechanism of thickening, especially if the screw dislocations are able to multiply by cross-slip over short distances under the combined applied and internal stress fields. It is implicit in Mahajan's suggestion that microslip must precede twin nucleation and must continue while the twin grows.

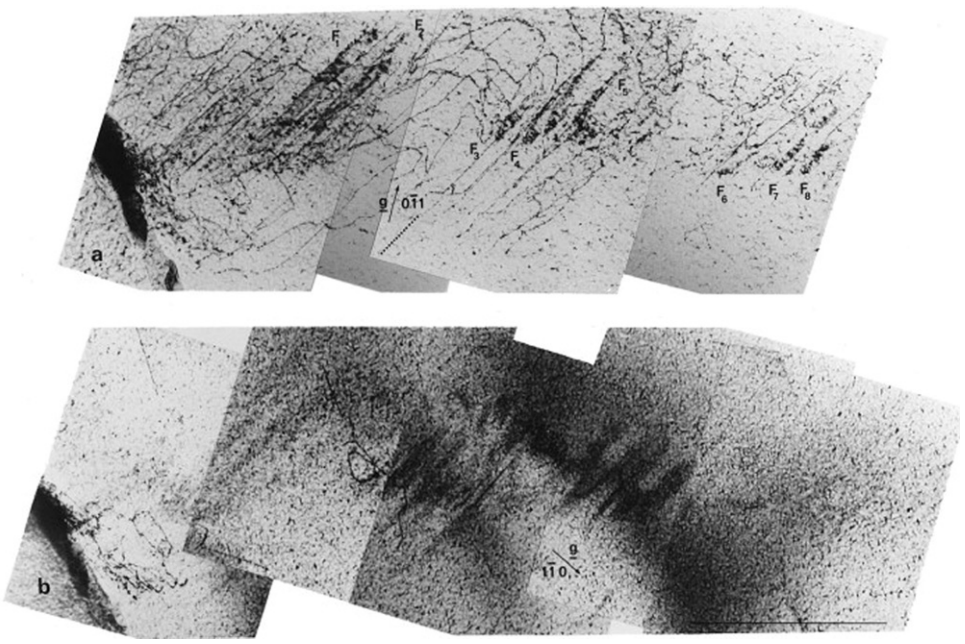

Figure 3 Micrographs showing faults F_1–F_8 and interspersed slip dislocations in deformed Fe–Cr–Co alloy for different operating reflections. The dashed line in (a) represents the projection of the Burgers vector of slip dislocations on the plane of the micrograph (Mahajan *et al.*, 1980).

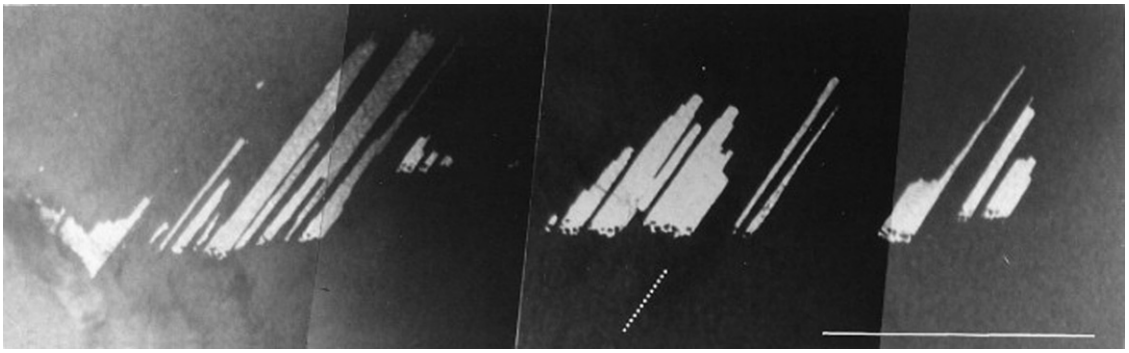

Figure 4 Dark-field image of faults shown in **Figure 3**. This shows that F_1–F_8 are twins. Again the dashed line represents the projection of the Burgers vector of slip dislocations on the plane of the micrograph (Mahajan *et al.*, 1980).

1.2 FCC Metals and Alloys and Related Structures

Cottrell and Bilby (1951) showed that their theory when applied to an analogous dissociation in f.c.c. metals and alloys would produce only a monolayer stacking fault because the glide of a $\frac{1}{6}\langle 11\bar{2}\rangle$ twinning partial is restricted to a particular $\{111\}$ plane. To obviate this problem, Venables (1961) suggested a modified mechanism to allow continuous thickening of a single fault, resulting in a microscopic twin.

Venables' model is schematically illustrated in **Figure 5**. Using the notation of the Thompson tetrahedron, consider a situation where a dislocation with Burgers vector **AC** lies in plane b except for a long jog N_1N_2 lying in plane a, as shown in **Figure 5(a)**. Assume that the part of the dislocation in plane a now dissociates into a Shockley and a Frank partial

$$\mathbf{AC} \rightarrow \mathbf{A\alpha} + \boldsymbol{\alpha}\mathbf{C} \qquad [3]$$

Under the action of the stress, the glissile Shockley partial $\boldsymbol{\alpha}\mathbf{C}$ moves away from the sessile Frank partial $\mathbf{A\alpha}$ on the a plane, leaving an intrinsic fault (**Figure 5(b)**). After attaining the unstable semicircular configuration $\boldsymbol{\alpha}\mathbf{C}$ winds rapidly around N_1 and N_2 to reach the position shown in **Figure 5(c)**. In this arrangement, two segments of the $\boldsymbol{\alpha}\mathbf{C}$ dislocation delineating the fault meet

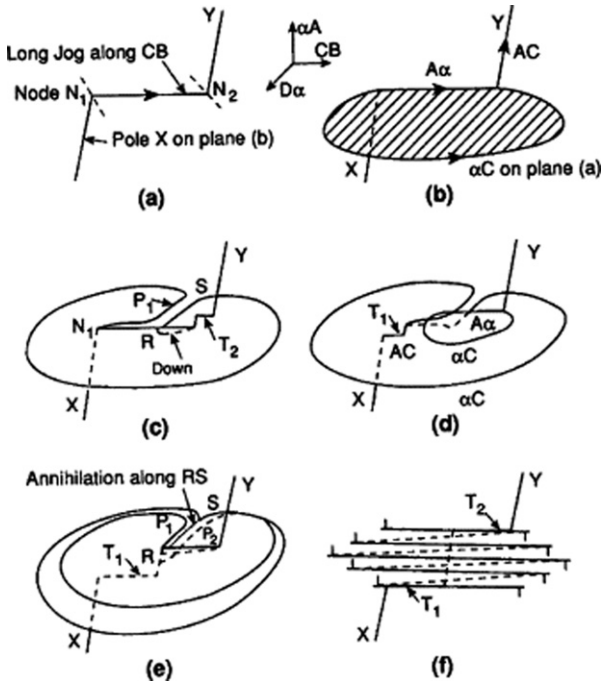

Figure 5 Prismatic glide mechanism for f.c.c. twinning (Venables, 1961).

along RS at a separation of only one interplanar distance. Since these two parts of **αC** are opposite in sense, a very large stress would be required to force them past each other.

Venables assumed that the end portion of the partial **αC** recombines with the sessile partial **Aα** along the length RN_2 and the reformed dislocation with Burgers vector **AC** then glides to the next plane a and repeats the dissociation. He showed that the repeated operation of these steps could lead to a microscopic twin as schematically illustrated in **Figures 5(c)–5(f)**. Later theories of deformation twinning in f.c.c. materials are based on the experimental result that twinning does not begin until slip is activated on at least two systems (Christian and Mahajan, 1995). The simplest description is that of Mahajan and Chin (1973a) who considered a reaction between dislocations of the primary system with Burgers vector **BC** and of the co-planar system with vector **DC** to form three Shockley partials

$$\mathbf{BC} + \mathbf{DC} \rightarrow 3\boldsymbol{\alpha}\mathbf{C} \qquad [4]$$

that are then rearranged on successive planes to form a three-layer fault. A small twin is obtained when embryonic three-layer twins at different heights in a slip-band grow together, an approach very similar to that of Mahajan for b.c.c. crystals.

Various steps of reaction [4] are schematically shown in **Figure 6**. Suppose two dislocations with Burgers vectors **DC** and **BC**, each dissociated into Shockley partials, glide on plane a. Reaction [4] is opposed by the mutual repulsion of **αC** and **Dα**. Mahajan (1975b) proposed that the repulsive interaction could be made attractive if at a constriction, **DC** dissociates so that **αC** lags behind **Dα**; the high-energy faults implied by this switch in positions may be avoided if the further dissociations $\boldsymbol{\alpha}\mathbf{C} \rightarrow \mathbf{B}\boldsymbol{\alpha} + \mathbf{D}\boldsymbol{\alpha}$ and $\mathbf{D}\boldsymbol{\alpha} \rightarrow \boldsymbol{\alpha}\mathbf{C} + \boldsymbol{\alpha}\mathbf{B}$ are assumed (see **Figure 6(b)**). The partials **Bα** and **αB** annihilate each other, leading to the formation of a fault-pair, as shown schematically in **Figure 6(c)**. It is not obvious how this fault-pair converts into a three-layer twin as implied by reaction [4].

Figure 7 is reproduced from the study of Mahajan and Chin (1973b) on the formation of deformation twins in f.c.c. crystals. The figure shows a tapering (111) twin F_1 with faults F_2–F_5 or dislocations L, M, and N ahead of it. Contrast experiments show that F_1 is bounded by two sets of partials and their Burgers vectors are $\frac{1}{6}[11\bar{2}]$ and $\frac{1}{6}[1\bar{2}1]$. The glide of the first set of partials may have formed F_1, whereas the second set of partials may be responsible for accommodating internal stresses that exist at a twin tip terminating within a crystal. The contrast behavior of F_2, F_4, and F_5 is consistent with the assignation of a full-vector to these faults that is parallel to $[11\bar{2}]$. Dislocations L and M have Burgers vectors $\frac{1}{2}[10\bar{1}]$ and $\frac{1}{2}[01\bar{1}]$. The contrast of dislocation N is complex and Mahajan and Chin concluded that its effective Burgers vector is $\frac{1}{2}[11\bar{2}]$ and that it consists of three closely spaced $\frac{1}{6}[11\bar{2}]$ dislocations. In this figure, **CD** and **GH** represent projections of the $[10\bar{1}]$ and $[01\bar{1}]$ vectors onto the (001) plane. Comparing these projections with those of various dislocations in **Figure 7**, it is inferred that the portions of dislocations L and M that react to form F_3 are in screw orientation, whereas the majority of M dislocations are nonscrew in character. Mahajan and Chin identified the crystallography of **Figure 7** as evidence that the twin F_1 is formed by a slip–twin conversion according to a reaction which is a

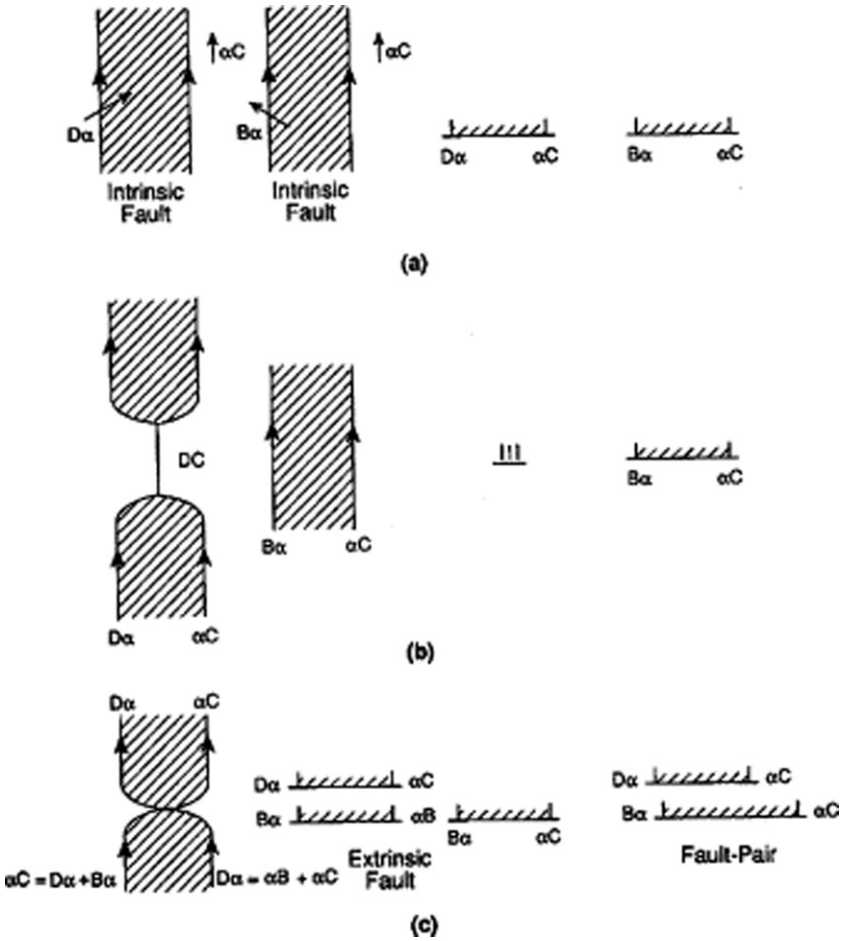

Figure 6 Schematic illustration of the formation of a fault pair in f.c.c. crystals (Mahajan, 1975a).

variant of eqn [4]. Similar indirect support for the Mahajan–Chin model comes from the observations of Robertson (1986) on a terminating twin and accompanying dislocations in nickel. The Burgers vectors of the twinning partials and of the whole dislocations were consistent with eqn [4].

Chin *et al.* (1969) examined the behavior of Co–Fe single crystals under constrained deformation. A specimen was oriented for $[1\bar{1}0](110)$ plane strain compression, i.e., the compression axis was [110] and the specimen was allowed to elongate along $[1\bar{1}0]$, but was prevented from widening along [001]. The imposed shape change was found experimentally to be achieved by a combination of the slip systems $[\bar{1}01](111)$, $[0\bar{1}1](111)$, $[0\bar{1}\bar{1}](11\bar{1})$, and $[\bar{1}0\bar{1}](11\bar{1})$ and twinning systems $[\bar{1}1\bar{2}](\bar{1}11)$ and $[\bar{1}12](\bar{1}1\bar{1})$. On the basis of the Mahajan–Chin model, the operative slip vectors could activate the two observed twinning variants, together with $[11\bar{2}](111)$ and $[112](11\bar{1})$ twins. However, these last two twins would elongate the crystal along [110] and thus would not be expected. To obtain the observed twin systems using Venables' and other models that are discussed in detail by Christian and Mahajan (1995), slip dislocations required for the formation of the observed twins cannot be activated either by the applied compressive stress along [110] or by the reaction stress along [001].

The presence of atomic order in the f.c.c. structure imposes crystallographic constraints on twinning. This is illustrated in **Figures 8** and **9** that show the projections of the $L1_2$ (A_3B alloy) and $L1_0$ (AB alloy) structures on to a (111) plane. In the disordered f.c.c. alloy, the twinning vectors on the (111) plane are **CD**, **CE**, and **CF**. However, the operation of these vectors in the $L1_2$ structure in **Figure 8** would lead to high-energy faults and order would not be preserved. On the other hand, if twinning occurs with a vector **GH** or its equivalent, then the order is preserved in the resulting twins. Twins can also be produced in the disordered f.c.c. alloy by consecutive displacements on (111) planes along **GH**. This implies that superalloys consisting of disordered f.c.c. matrix and particles having the $L1_2$ structure can undergo compatible deformation by twinning using the vector **GH** or its equivalent.

When the $L1_0$ order is present, one of the twinning vectors of the disordered lattice can produce twins in the ordered structure, for example **IJ** in **Figure 9**. The operation of vectors **LK** and **MK** can also lead to twinning. It is clear from **Figures 8** and **9** that the presence of order imposes additional constraints on the occurrence of twinning.

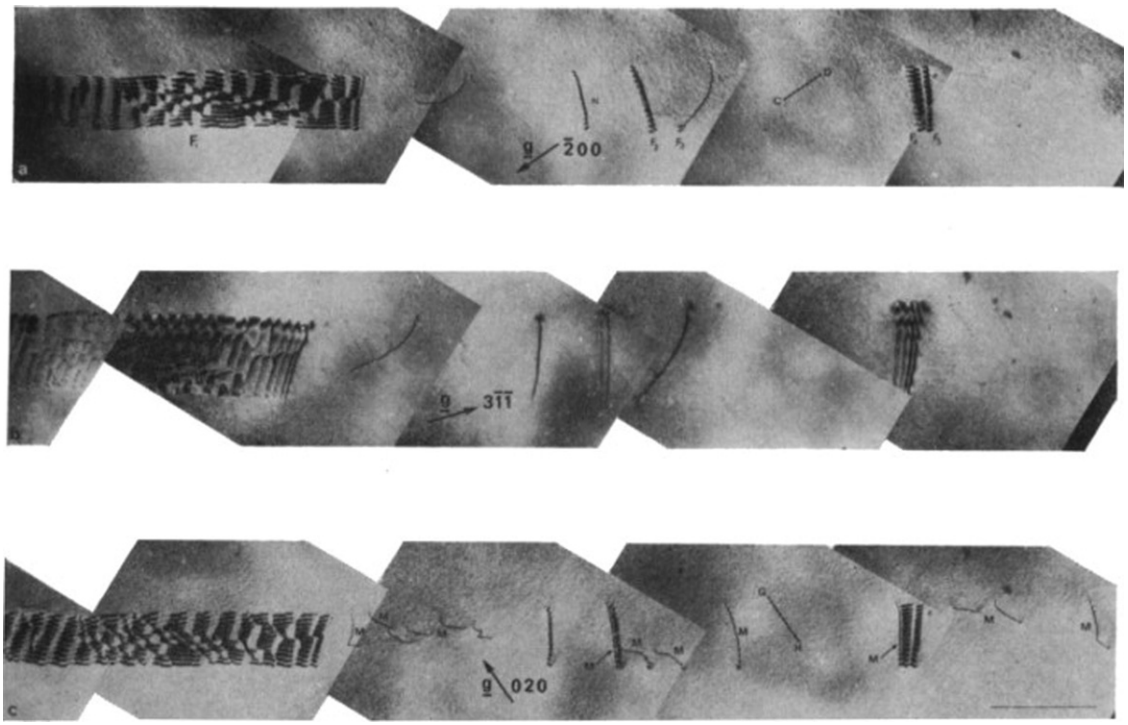

Figure 7 Micrographs illustrating the contrast behavior of dislocations and faults observed ahead of a twin F_1 in a deformed Co–9.5 wt% Fe alloy deformed at 77 K. The planes of the micrographs are (a) ~(001), (b) ~(112), and (c) ~(001). CD and GH are the projections of the $[10\bar{1}]$ and $[01\bar{1}]$ vectors on the (001) plane. The marker represents one micron (Mahajan and Chin, 1973a).

Dislocation models (Yoo, 1997; Cerreta and Mahajan, 2001) have been developed to rationalize the formation of deformation twins in the $L1_0$ structure. Yoo (1997) proposed a pole model, which is conceptually analogous to Venables' mechanism for f.c.c. twinning. Cerreta *et al*. have extended the Mahajan–Chin model (Mahajan and Chin, 1973a) to twinning in the $L1_0$ structure. Their suggestion is illustrated in **Figure 10** and involves a reaction between a super dislocation **2CB** and an ordinary dislocation **BA**. **Figure 10(a)** shows that the super dislocation **2CB** is dissociated into two superpartials $2C\delta$ and $2\delta B$ and a superlattice intrinsic stacking fault (SISF) separates the two partials. It can be shown that if the dissociated super dislocation meets the ordinary dislocation BA as shown in **Figure 10(b)**, a fault-pair consisting of three Shockley partials **Cδ** would form as depicted in **Figure 10(c)**; SESF refers to superlattice extrinsic stacking fault. Cerreta and Mahajan (2001) assumed that twins thicken by the coalescence of fault-pairs located at different heights within slip bands. Their results on twinning in TiAl tend to support the proposed model.

1.3 h.c.p. Materials

Twinning in h.c.p. materials was reviewed by Yoo (1981), and **Figure 11** shows his plot of twinning shear (g) vs. c/a for the main twinning modes, with the observed modes of seven h.c.p. metals superimposed. The $\{10\bar{1}2\}$ mode is found in all cases. If a uniaxial tensile stress is applied along the c axis, twins of a particular mode may form if the mode line in **Figure 11** has a negative slope, whilst a crystal or grain subjected to compression along its c axis may twin only if the line has a positive slope. This rule is reversed for the two conjugate modes, listed on the same plots as their primary modes. Thus, with respect to the c axis, $\{11\bar{2}1\}$ is a 'tension' twin, $\{11\bar{2}2\}$ and $\{10\bar{1}1\}$ twins are 'compression' twins. The $\{10\bar{1}2\}$ twin is a compression twin for Cd and Zn, whereas it is a tension twin for all other metals.

Thompson and Millard (1952) independently suggested a pole model for the formation of $\{10\bar{1}2\}$ twins in h.c.p. metals and alloys. The twinning dislocation is a zonal type of double step height. According to their mechanism, a 'major' dislocation of Burgers vector $[000\bar{1}]$ lying on the $(10\bar{1}2)$ plane of the matrix could be incorporated into a $\{10\bar{1}2\}$ twin, where it becomes a sessile dislocation with a $10\bar{1}0$ Burgers vector in the twin lattice, and it then leaves a double step in the interface. Thompson and Millard apparently treated the pole dislocation and the twin nucleus as distinct defects that interact, and they apparently did not explicitly consider a combined nucleation and growth mechanism from an initial dissociation of a single dislocation.

In addition, as twin nucleation is an atomic scale phenomenon, recent atomic scale calculations (Wang *et al*., 2009a, 2013) suggest that in h.c.p. materials twins nucleate as multi-layers, rather than the motion of single twinning dislocations as suggested in the pole mechanism (Thompson and Millard, 1952). The twin that has received the most attention is the $\{10\bar{1}2\}$ twin, which is the most frequently observed twin among all the h.c.p. metals. A single twinning dislocation of this twin spans two atomic twin

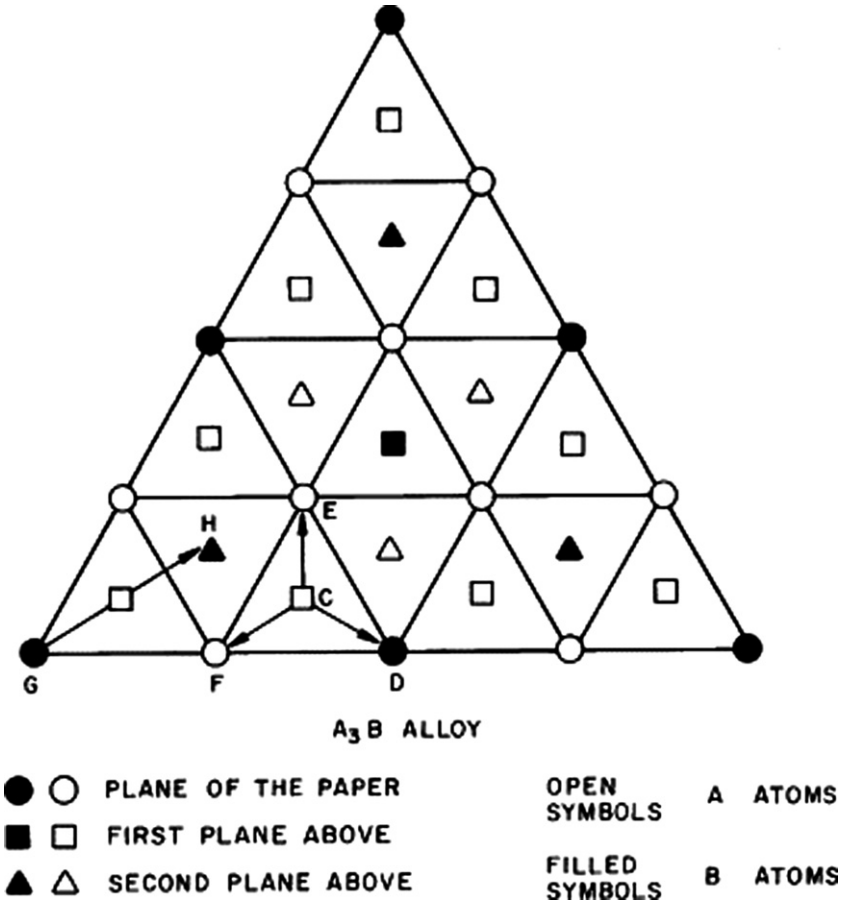

Figure 8 Schematic showing the projection of the $L1_2$ structure on to a (111) plane.

planes or layers. Unlike in f.c.c. and b.c.c. metals, the twin orientation in h.c.p. metals cannot be completely achieved via shearing by the glide of twinning dislocations. It requires supplementary atomic shuffling – atomic movements that vary in direction and distance.

In f.c.c. metals, a twinning dislocation belonging to an f.c.c. metal can glide in a perfect f.c.c. crystal and create a stable monolayer twin fault. A two- or three-layer f.c.c. twin can be constructed by sequential glide of twinning dislocations on adjacent twin planes (Zhu *et al.*, 2012; Mahajan, 2013). In contrast, it has been shown via atomic scale calculations that a single $\{10\bar{1}2\}$ twinning dislocation cannot glide alone in a perfect h.c.p. crystal. Accordingly, unlike twin nuclei in f.c.c. metals, the $\{10\bar{1}2\}$twin nuclei in h.c.p. metals cannot be constructed via sequential layer-by-layer glide of individual twinning dislocations. This finding also indicates that a stable $\{10\bar{1}2\}$ twin embryo must consist of more than two layers. In this regard, atomic-scale calculations have shown that the stable $\{10\bar{1}2\}$ twin nucleus contains at least six atomic layers or at least three twinning dislocations (Wang *et al.*, 2009b). These results also suggest that twin nucleation is energetically less likely to occur within the grain than the grain boundaries since formation of a multi-layer twin embryo is required. This conjecture is consistent with microstructural characterization of deformed h.c.p. metals that find that twins appear to originate from grain boundaries (see Section 4.1).

The minimum number of layers for a stable nucleus is not likely to be the same for all types of h.c.p. twins. However, the structure of the twin nuclei of only very few twin types have been studied. For example, the Burgers vector of an elementary twinning dislocation for the $\{11\bar{2}1\}$ twin mode is about $\frac{1}{36}\langle 11\bar{2}6\rangle$ in cobalt. Therefore, Vaidya and Mahajan (1980) suggested that the following reaction of two $\frac{1}{3}\langle\bar{2}11\bar{3}\rangle$ dislocations with a $\langle 1\bar{1}00\rangle$ dislocation would yield a 12-layer $\{11\bar{2}1\}$ stable twin nucleus.

$$2\times\tfrac{1}{3}\langle\bar{2}11\bar{3}\rangle+\langle 1\bar{1}00\rangle\rightarrow 12\times\tfrac{1}{36}\langle 11\bar{2}6\rangle \qquad [5]$$

The $\langle 1\bar{1}00\rangle$ dislocations might arise from interactions between $\frac{1}{2}\langle 11\bar{2}0\rangle$ dislocations. The mechanism is thus similar in concept to that suggested by Mahajan and Chin (1973a) for f.c.c. twinning.

Multi-atomic layer $\{10\bar{1}2\}$ twin nuclei are believed to form via atomic shuffling. Lann and Dubertret (1979) and Dubertret and Le Lann (1980) proposed that formation of the reoriented structure of the twin embryo involved atomic shuffling. Shuffling

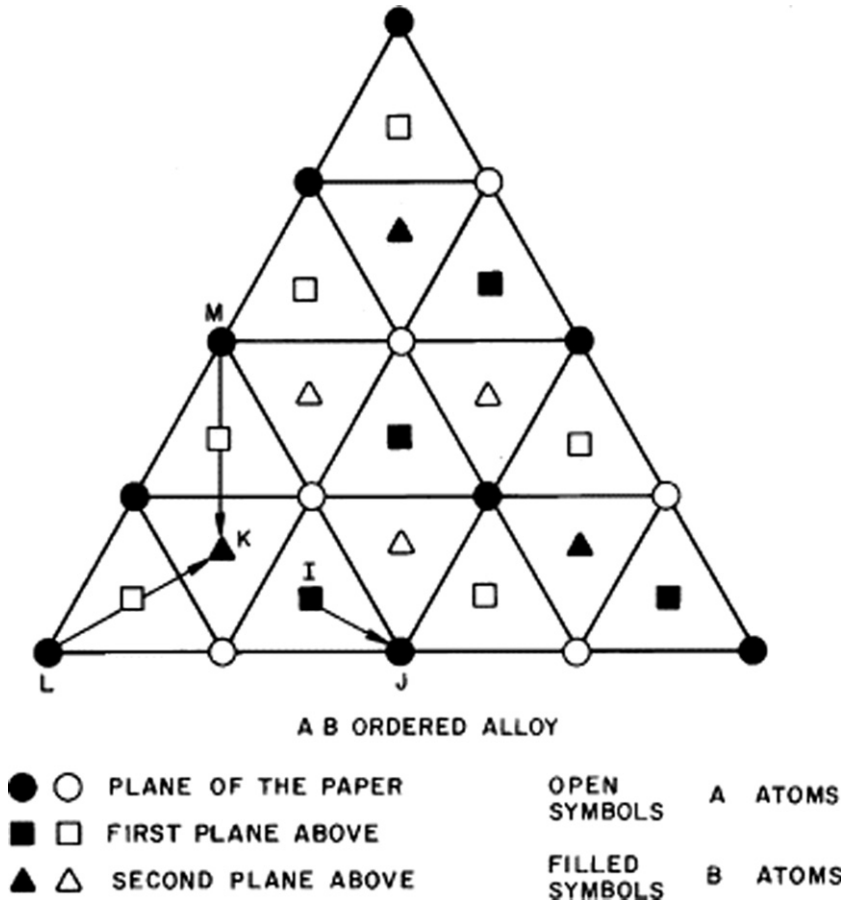

Figure 9 Schematic showing the projection of the $L1_0$ structure on to a (111) plane.

enabled transformation of the basal plane in the untwinned crystal to the prismatic plane in the twinned one. This pure-shuffle model for nucleation of $\{10\bar{1}2\}$ twins has been supported by indirect experimental evidence, such as TEM observations of prismatic/basal (PB) boundaries or lack of emissary twins (Song and Gray III, 1995a), and MD observations in atomic-scale simulations (Li and Ma, 2009; Wang *et al.*, 2013; Xu *et al.*, 2013).

While initial creation of a twin requires formation of a multilayered embryo, the growth of twin can proceed by layer-by-layer glide of single twinning dislocations on twin boundaries. One source for twinning dislocations is the dissociation reaction that takes place when a lattice dislocation runs into the twin boundary (Serra *et al.*, 1991; Serra and Bacon, 1996; Wang *et al.*, 2012). The reaction produces a twinning dislocation (disconnection) or dislocations of the same variant as the twin boundary, which can glide away from the reaction site, advancing (or shrinking) the twin. This growth mechanism applies to all twins and has been seen in atomic scale simulations for many twin types. If the Burgers vectors of the lattice and twinning dislocations are denoted by b_1 and b, respectively, then the reaction can be written as $b \rightarrow b_R + b_1$, where b_R is the residual dislocation. Whether this dissociation reaction can take place depends on the energy to split the atomic core of the impinging dislocation as well as a few necessary but not sufficient geometric rules. These basic rules are (1) the line of the dislocation b must coincide with the line of intersection of the slip plane n and twinning plane n_T, (2) the Burgers vectors must be conserved, e.g., $b - b_R + b_1 = 0$, and (3) the interaction forces between the twinning dislocation(s) and the residual dislocation are repulsive.

When the loading direction changes from one direction to another, such as in cyclic loading or when loading in tension a material that had be previously rolled, a phenomenon called de-twinning may occur. In de-twinning, twins gradually disappear with straining. Consequently, the alterations in slip caused by the reoriented twinned domains and presence of twin boundaries can be concomitantly removed as well. In this way, de-twinning can lead to changes in the yield stress and in the evolution of the flow stress and hardening rate. De-twinning has been observed in Mg, Zr, and Be (Lou *et al.*, 2007; Wu *et al.*, 2007; Proust *et al.*, 2010; Brown *et al.*, 2013).

Detwinning may occur by internal twinning within the original twin. Indirect experimental evidence suggests that the stress to detwin a twin is higher stress than that to grow the twin (Partridge, 1967; Brown *et al.*, 2013). When the twin forms during forward loading, defects can accumulate within its domain and the twin boundary can become offset from its ideal orientation. These alterations can make detwinning more difficult than twinning.

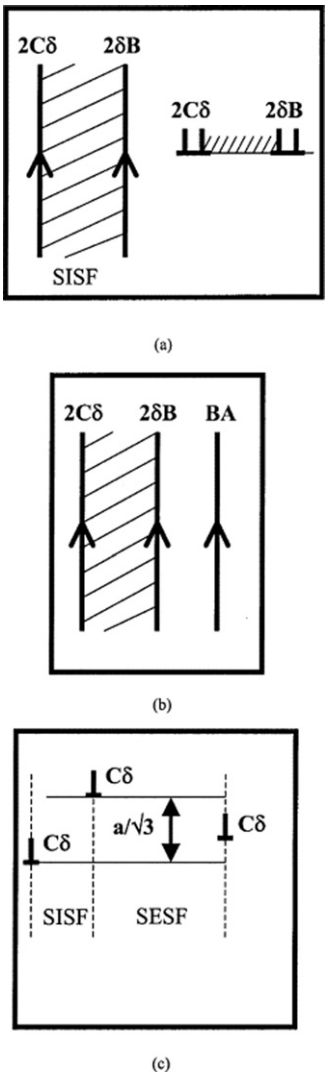

Figure 10 Schematic illustrating the formation of a fault-pair in the $L1_0$ structure (Cerreta and Mahajan, 2001)

2 Influence of Material Variables on Twinning

It is beyond the scope of this article to review in detail the influence of material variables on deformation twinning. Therefore, we have chosen to limit the discussion to a few variables the influence of which may be rationalized in terms of the twin formation mechanisms discussed earlier: (i) temperature, (ii) strain rate, (iii) prestrain, and (iv) microstructure of polycrystals, i.e., grain size, texture, etc.

2.1 Temperature

The propensity of twinning in most b.c.c., f.c.c., and h.c.p. metals and alloys increases as the deformation temperature is lowered. On the other hand, twinning in TiAl becomes active at temperatures around 750–800 °C where slip by ordinary and superlattice dislocations takes place, but not at lower temperatures where glide by superlattice dislocations dominate (Cerreta and Mahajan, 2001). This observed temperature dependence of twinning in TiAl is unusual as compared to those of other metals and alloys.

It is well accepted that as the deformation temperature is lowered, screw dislocations constitute a major component of deformation-induced substructure in b.c.c. metals and alloys. This is so because the mobility of screw dislocations is reduced on lowering the temperature due to their nonplanar, complex core structure. This feature is also responsible for the strong temperature dependence in yield strength exhibited by most b.c.c. metals and alloys. If we invoke that screw dislocations are a pre-requisite for the formation of twins (Sleeswyk, 1963; Mahajan, 1972a, 1975a) in b.c.c. materials, then the observed increase in twinning frequency with the decreasing temperature can be rationalized.

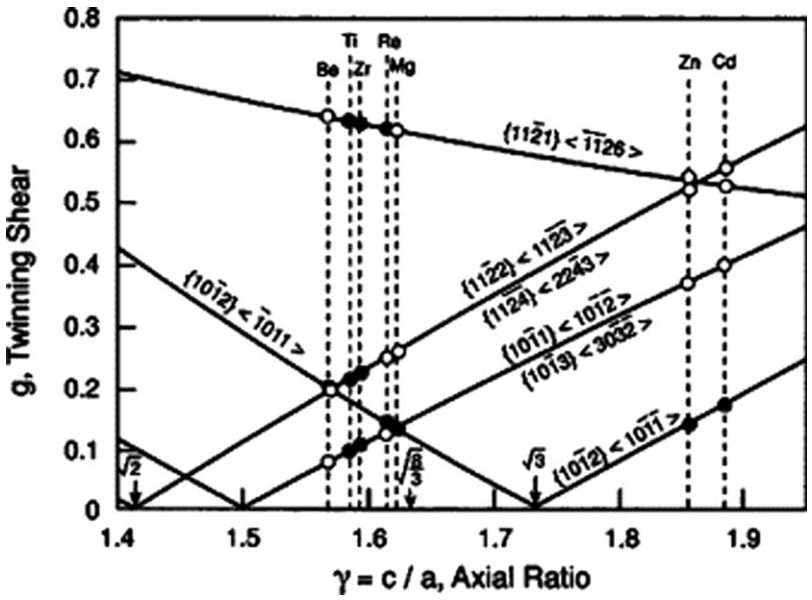

Figure 11 Variation of twinning shear with the axial ratio for the seven hexagonal metals. A filled symbol indicates that the twin mode is an active mode (Yoo, 1981).

It is implicit in the models of Sleeswyk and Mahajan that slip precedes twinning. An interesting question is why does not deformation continue to occur exclusively by slip? There is no clear-cut answer to this difficult question. It is conceivable that the distribution of dislocations within a microslip band is such that deformation by twinning is favored over that by slip because the bypass stress for twinning partials is lower than that for slip dislocations.

In f.c.c. metals and alloys, temperature affects not only the competition between slip and twinning, but also the type of twin that is formed. Alloys with very low fault energies may at low temperatures undergo localized twinning on a very fine scale. At higher temperatures, or with higher fault energies, conventional large twins may form. There is sometimes an intermediate range in which bands of local flow contains twins on the primary and conjugate slip systems.

The careful work of Suzuki and Barrett (1958) on single crystals of silver-gold alloys of different compositions but fixed orientation established three regimes similar to those described above. Their results are shown in **Figure 12**. In region I a localized band of twins has formed on the primary or conjugate slip planes. This is followed by a second band of twins on the other (conjugate or primary) planes. Twinning is accompanied by load drops. In region II twin bands form on either the primary or the conjugate planes in different parts of the specimen, and grow until they impinge on each other. In region III, which was found only in silver-rich alloys at low temperatures, twins form extensively on both primary and conjugate planes, and there are no sharp load drops.

The results of Suzuki and Barrett (1958) appear to be consistent with the model of Mahajan and Chin (1973a). In region I the probability of cross-slip is high. As a result, the glide dislocations involved in the formation of embryonic twins could undergo double cross-slip, and could react to form twins at different heights within slip bands. The coalescence of these twins could lead to thicker twins and concomitant load drops. However, when the temperature is low, double cross-slip may not occur, and thus thin twins may be produced. Furthermore, it can be argued that the effect of reduced temperature on twinning may be analogous to that of reduced stacking fault energy because both parameters reduce the incidence of double cross-slip.

The observed temperature dependence of twinning in TiAl may be rationalized in terms of the model of Cerreta and Mahajan (2001). Their model requires both ordinary and superlattice dislocations for the formation of fault-pairs, which serve as embryonic twins. These dislocations are indeed observed in the temperature range where twinning occurs.

Twinning in polycrystalline h.c.p. metals and alloys often arises because of the lack of an adequate number of slip systems to accommodate an imposed strain. The measured twinning stress decreases slightly with decreasing temperature for most h.c.p. modes, except for $\{10\bar{1}1\}$ twinning, where an increase has been reported (Knezevic *et al.*, 2015). In polycrystalline Zr, room-temperature deformation at moderate strain rates is accomplished mainly by $\{10\bar{1}1\}$ prismatic slip and $\{10\bar{1}2\}$ twinning, together with infrequent $\{11\bar{2}1\}$ twins (Christian and Mahajan, 1995). At 77 K, the amount of $\{10\bar{1}2\}$ twinning was considerably increased and there were many more $\{11\bar{2}1\}$ twins and also some $\{11\bar{2}2\}$ twins.

2.2 Strain Rate

Strain rate and temperature effects in materials are usually coupled by an Arrhenius type equation, which is characteristic of a thermally activated process. A rapid change of some property with temperature then indicates that the same property has a high

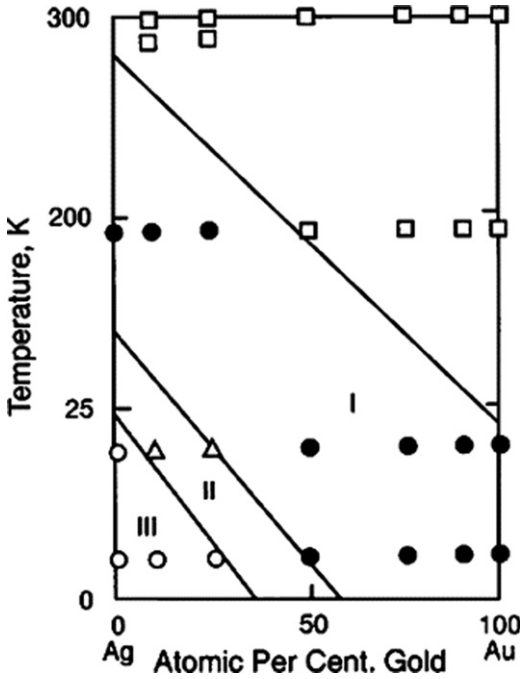

Figure 12 Temperature-composition diagram showing the occurrence of twinning in Ag–Au alloys. In region I, twinning occurs on the primary slip plane. In region II, twins are observed on the primary as well as on the conjugate planes but in different regions. In region III the two types of twins coexist in the same region. Failure to twin in the main part of the specimen is denoted by the squares (Suzuki and Barrett, 1958).

sensitivity to an imposed rate, and vice versa. The expected general equivalence of high strain rates and low temperatures is certainly valid for twinning. Indeed, under shock loading or severe impact conditions, all b.c.c., f.c.c., and h.c.p. materials can deform predominantly by twinning. f.c.c. materials with high stacking fault energies, especially aluminum alloys, do not twin under normal deformation conditions, but twinning has been observed in shock-loaded Al–Mg alloys (Gray III, 1988).

A characteristic structure after shock loading of iron consists of a uniform distribution of long screw dislocations. This is quite different from the tangled dislocation structures found after room temperature deformation at normal strain rates, but is very similar to structures, consisting of long screw dislocations, observed after deformation at low temperatures. As discussed earlier, the immobile screw dislocations could dissociate into twin embryos.

As noted above, the increase in strain rate also accentuates the formation of twins in f.c.c. metals and alloys. Since the incidence of double cross-slip is reduced, the probability of interaction between coplanar dislocations required according to the Mahajan–Chin model should be increased, resulting in thin twins. This effect is analogous to that of low temperature on twinning in f.c.c. materials that is discussed above.

2.3 Pre-strain

There are numerous observations in the literature that show that twinning in a number of b.c.c. metals can be suppressed by a strain previously applied at a higher temperature (Christian and Mahajan, 1995). Furthermore, the amount of pre-strain needed to suppress twinning depends on the strain rate subsequently imposed, and the twinning behavior of pre-strained iron can be restored by aging (Christian and Mahajan, 1995).

A cogent explanation for the above observations is that screw dislocations are necessary for the formation of twins in b.c.c. crystals. At pre-strain temperatures, screw dislocations are mobile because their cores are not extended. As a result, dislocation cell structures develop during pre-straining. During subsequent deformation at low temperatures, the glide of dislocations in the cells accommodates the imposed stress. Since these dislocations are non-screw in character, they cannot evolve into embryonic twins. However, if we impose aging after pre-straining, impurities could migrate to dislocations constituting cell walls. As a result, these dislocations get pinned and do not actively participate when the material is subsequently deformed at a low temperature. This constraint allows the evolution of deformation substructure that is characteristic of low temperature, i.e., well-aligned, long screw dislocations. These screw dislocations can then evolve into embryonic twins during the low-temperature deformation.

2.4 Grain Size and Texture in h.c.p. Materials

h.c.p. Polycrystalline metals are typically processed by a series of bulk mechanical processes, such as forging, rolling, swaging, and forming, in order to refine the initially cast microstructure or to shape it into a basic form, such as a sheet or rod. These

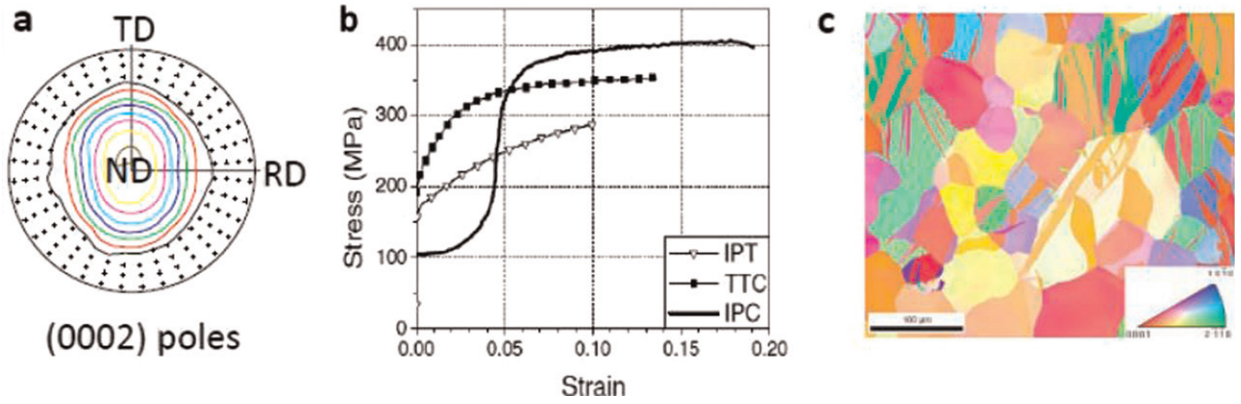

Figure 13 AZ31 Mg deformed at 300 K and 10^{-3} s^{-1}. (a) {0002} basal pole distribution of the initial rolling texture, showing a sharp texture of highly oriented basal poles near the Normal Direction (ND) to the plate; (b) stress–strain response of samples deformed by In-Plane Tension (IPT), In-Plane Compression (IPC) and Through Thickness Compression (TTC); (c) EBSD micrograph showing $\{10\bar{1}2\}$ tensile deformation twins (Proust *et al.*, 2009).

processes often cause the metal to develop a strong texture, in which a majority of the grains have reoriented in nearly the same direction.

Figure 13(a) shows the texture of an Mg alloy sheet (AZ31) after it has been rolled. The texture is shown using a {0002} basal pole figure, where the orientations of the c-axes of all the grains in 3D space are projected onto a 2D plane. As shown, a majority of the c-axes (basal poles) have preferentially aligned along the Normal Direction (ND) of the plate. This strong texture is typical of most h.c.p. metals that have been rolled to large strains.

Sharp h.c.p. textures, such as the one shown in **Figure 13(a)** for AZ31 Mg, are expected to significantly affect the material constitutive response. **Figure 13(b)** shows the corresponding stress–strain responses of this material when deformed either In Plane (IP) along the rolling direction (RD), in tension or compression, and through the thickness (TT) of the sheet along the ND. The response is seen to be highly plastically anisotropic, in which the flow stress and hardening rates highly depend on the direction and sense of loading. The high degree of plastic anisotropy is typical of h.c.p. metals and is a result of the strong orientation dependence of deformation twinning (Beyerlein *et al.*, 2011).

Twinning is directional, activated either when the *c*-axis is subject to tension or compression. For the $\{10\bar{1}2\}$ extension twin type studied in **Figures 13(b)** and **13(c)**, twinning is activated in grains subject to c-axis tension. Thus, whether $\{10\bar{1}2\}$ twinning is activated in a polycrystalline material depends on the orientation relationship of the grains (texture) and the stress state applied to the material. For instance, in **Figure 13(b)**, in In-Plane Tension (marked as IPT), the tensile axis relative to the basal poles of most grains places the *c*-axis of the grains in compression. This orientation favors slip over twinning. Therefore, the IPT flow stress increases with strain with a slow decreasing hardening rate, characteristic of slip-dominated flow. This response is typical of the plastic deformation response of many metals that deform predominantly by slip.

In the case of In-Plane Compression (IPC) because the relative orientation of basal poles and the compression axis places the c-axes of the grains in tension, tensile $\{10\bar{1}2\}$ twinning is favored. In the early stages of IPC deformation, deformation twins form in many grains and with further straining, they expand into domains that can be large relative to the grain size (see **Figure 13(c)**). Under IPC, these twin-reoriented regions are 'hard-to-deform' relative to the original parent orientation. Thus, as the twin volume fraction increases, the material as a whole becomes harder to deform. Twinning results in the increase in hardening rate with straining seen in the IPC stress–strain curve.

Twinning plays a major role in the evolution of texture during mechanical loading by altering the lattice orientation in portions of the grains. The most common h.c.p. twin, $\{10\bar{1}2\}$ twinning, is one of the best examples of this phenomenon. **Figure 14** shows the evolution of texture of pure Zr under In-Plane Compression (IPC) (Niezgoda *et al.*, 2014). These textures are presented in the form of {0002} pole figures. The initial material was twin-free and its texture was highly oriented and similar to that shown in **Figure 14(a)** with the *c*-axis of most of the grains nearly parallel to the ND of the sheet. When strain in the IPC direction (the rolling direction, RD, in the figure) is applied and increased, $\{10\bar{1}2\}$ twinning is activated and the volume fraction of twinned material increases. Within the $\{10\bar{1}2\}$ twinned regions, the c-axis reorients by $\sim 86^\circ$ relative to the original orientation in the grain, which corresponds to a decrease in the density of {0001} poles along ND and correspondingly an increase in their density along the RD. As shown in **Figure 14**, this reorientation of the basal poles by twinning is not apparent at 4% strain, but starts appearing at 9% and becomes significant at 14% strain and higher. A similar change in texture occurs for other types of h.c.p. twins, such as $\{10\bar{1}1\}$ twinning or $\{11\bar{2}2\}$ twinning, although the amount of c-axis reorientation is lower than that of $\{10\bar{1}2\}$ twinning.

While twinning can have a significant impact on texture, texture measurements cannot be used to indicate the presence or onset of deformation twinning. When twins first form, they are relatively thin and fine compared to the parent grain size and the total volume of twins within the polycrystal is small. For instance in **Figure 14**, although the texture after 4% IPC strain does not exhibit

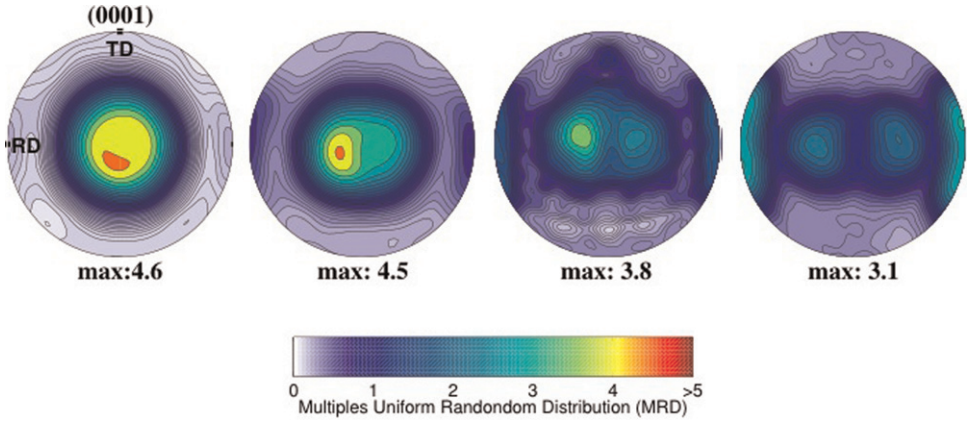

Figure 14 Zr deformed at 76 K and 10^{-3} s^{-1}. Evolution of texture in pure Zr as it is being compressed in the In-Plane Compression (IPC) direction. As the strain level increases, the volume fraction of $\{10\bar{1}2\}$ twins increases. Figure is taken with permission from Niezgoda *et al.* (2014).

the '*c*-axis reorientation' signature of twinning, twins have already nucleated. Microstructural characterization by electron backscattered diffraction (EBSD) of the same deformed material shows that at 5% strain, most of the grains, ~60% of them, have formed twins, yet the total twinned volume fraction in the material is only 5%. Texture measurements, like those shown in **Figure 14**, typically aim to include several thousands of grains. Twinning must reach a certain twin volume fraction (e.g., >10%) before they can have any substantial impact on the texture evolution of a bulk, polycrystalline metal.

In addition to the crystallographic orientation of the grain, the size of the grain is also known to affect the propensity for twinning. For f.c.c., b.c.c., and h.c.p. metals alike, twinning becomes more probable in the polycrystal as its average grain size increases, e.g., Zn (Armstrong *et al.*, 1962; Song and Gray, III 1995a, 1995b), Ti (Okazaki and Conrad, 1973), and Mg and Mg alloys (Agnew *et al.*, 2003; Barnett *et al.*, 2004; Barnett, 2008; Lentz *et al.*, 2014). Similarly, in a polycrystalline material containing a very broad range of grain sizes, more twins develop in the larger grains (Capolungo *et al.*, 2009; Beyerlein and Tome, 2010). Consequently, a twin is more likely found in the bigger grains of a polycrystalline sample. In h.c.p. metals, twins can differ in crystallography (see Section 1.3). Sensitivity of twinning to grain size depends on the type of twin. For instance, in Mg and Mg alloys, $\{10\bar{1}2\}$ tensile twins are found to be less sensitive to grain size than $\{10\bar{1}1\}$ compression twins (Lentz *et al.*, 2014). The reason for the grain size effect on twinning is being intensely studied, but has yet to be clarified. One prevailing thought is based on the notion that twins nucleate from defects (such as slip dislocations). Accordingly, the larger grains contain more twins because they have larger grain boundary areas and larger grain volumes and, thus, more potential nucleation sites (Beyerlein and Tome, 2010).

3 Accommodation of Deformation Twins and their Role in Crack Nucleation

It is apparent from the preceding discussion that slip and twinning may occur concomitantly in most single crystals and polycrystalline materials. It is then easy to visualize a number of situations where stress concentrations could develop during deformation: (i) a twin terminating within a crystal, (ii) a twin terminating on another twin, and (iii) a twin terminating on a sub-boundary or a grain boundary. A number of investigators have evaluated these different situations in b.c.c., f.c.c., and h.c.p. materials, and the reader is referred to the review by Christian and Mahajan (1995) for appropriate references.

The conceptual framework for analyzing different situations listed above in various crystal structures is based on Sleeswyk's elegant idea on emissary slip (Sleeswyk, 1963). He argued that emissary slip dislocations result from twinning partials that bound non-coherent twin boundaries. Therefore, the three types of interactions listed above are equivalent to the propagation of slip ahead of a terminating twin, across an existing twin, and across a grain boundary.

In b.c.c. crystals, the slip and twinning directions coincide and the twin plane is a frequently observed slip plane. This simplifies the problem of plastic accommodation and exact continuation of the twinning shear is possible. **Figure 15** due to Sleeswyk provides evidence for the propagation of the shear ahead of a stopped twin at A. A sub-boundary ahead of the twin acts as a 'marker' and is seen to have been sheared at B. Sleeswyk visualized that the observed shearing is caused by emissary slip that emanates from the terminating twin. The source of emissary slip is $\frac{1}{6}[111]$ twinning partials that bound the twin interface, and slip dislocations arise as a result of the reaction

$$\tfrac{1}{6}[111] \rightarrow \tfrac{1}{3}[\overline{111}] + [111] \qquad [6]$$

Sleeswyk envisaged that in a group of three twinning partials, only one of the partials dissociates according to eqn [6]. As a result, the effective Burgers vector of the non-coherent twin interface is close to zero, and the resulting interface has low energy.

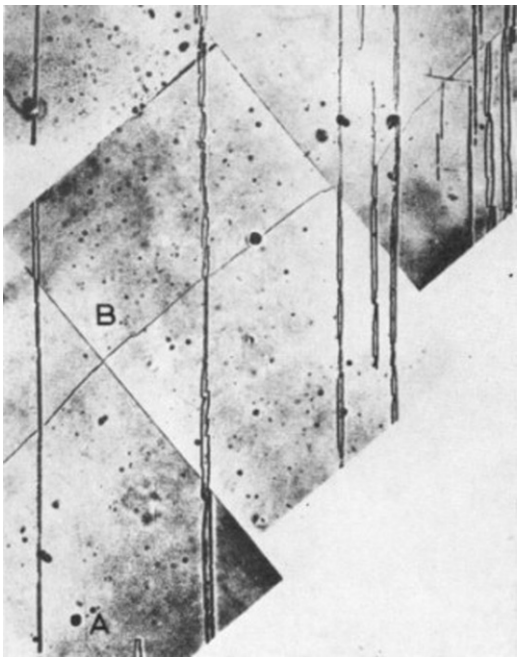

Figure 15 Deformation twins formed in pure Fe during compression at 77 K showing the displacement of a sub-boundary at B ahead of a twin which stopped at A (Sleeswyk, 1962).

Extensive studies have shown that although slip at the tips of twins in b.c.c. materials is frequently observed, the actual accommodation processes may be more complex. Hull (1963) found that in Fe–Si alloy the slip direction was always the same as the twinning direction, but the slip frequently takes place on {110} planes containing this direction. In a detailed study of slip patterns in a Mo–35 at% Re alloy, Mahajan (1972a) found evidence for both simple emissary slip on the twinning plane, as in the Sleeswyk model, and for slip on two planes, which was then not confined to the region directly ahead of the twin. However, the slip near some twins was much more complex and dislocations with Burgers vectors not parallel to the twinning direction were involved.

If we invoke that slip dislocations will form when a propagating twin is blocked, then twin–slip and twin–twin interactions are equivalent. Twin–slip and twin–twin interactions were extensively investigated in b.c.c. and f.c.c. crystals (Christian and Mahajan, 1995). It was found that during twin–twin interactions the strain of a crossing twin is propagated across a crossed twin by either slip or twinning. We have chosen an example each that involves accommodation slip and twinning to highlight these observations.

Twin–twin interactions in b.c.c. crystals can be classified according to the lines of intersection between crossing and crossed twins. Using this classification there are five types of intersections: ⟨111⟩, ⟨110⟩, ⟨120⟩, ⟨351⟩, and ⟨311⟩. **Figure 16** shows a ⟨120⟩ interaction in which the barrier twin (T_3) is $(2\bar{1}1)$ and the crossing twin is (211) so that the twins intersect along $[10\bar{2}]$ (Mahajan, 1971). Mahajan found the slip plane to be (10, 1, 5) of the matrix, which is equivalent to $(2\bar{3}1)_T$ of the barrier twin. If the formation of emissary dislocations is assumed, then the propagation of twinning strain of the crossing twin across the crossed twin by slip can be rationalized according to the reaction

$$3 \times \tfrac{1}{6}[\bar{1}11]_{(211)} \rightarrow \tfrac{1}{6}[\bar{1}51]_{(10,1,5)} + \tfrac{1}{3}[\bar{1}\bar{1}1]_{(2\bar{1}\bar{1})} \qquad [7]$$

where

$$\tfrac{1}{6}[\bar{1}51]_{(10,1,5)} = \tfrac{1}{2}[111]_{(23\bar{1})}\mathrm{T} \qquad [7a]$$

The crossing twin intersects the crossed twin along the $[10\bar{2}]$ direction, and its strain is propagated across the crossed twin by slip on the slightly unusual $(2\bar{3}1)_T$ plane. The observed slip plane in the twin satisfies the geometrical condition that the activated slip plane should contain the line of intersection of the crossing and crossed twins. This allows the movement of emissary dislocations associated with the crossing twin onto slip planes within the crossed twin without undergoing reorientation at the cross twin/crossed twin interface. Furthermore, the complementary dislocation $\frac{1}{3}[\bar{1}\bar{1}1]$, if stable, forms a double step in the coherent interface of the crossed twin. The decomposition is energetically unfavorable, but could occur when the stress concentration at the head of a pile-up of dislocations on the (211) plane of the crossing twin reaches a sufficient value.

Mahajan and Chin (1973b, 1974) found examples of shear propagation by both slip and secondary twinning in Co–8 wt%Fe single crystals, which had undergone a constrained, plane-strain deformation. **Figure 17**, taken from the study of Mahajan and Chin (1974), shows that the matrix is heavily twinned on $(\bar{1}1\bar{1})$ planes, marked T_1 on the micrograph, and the contrast shows that

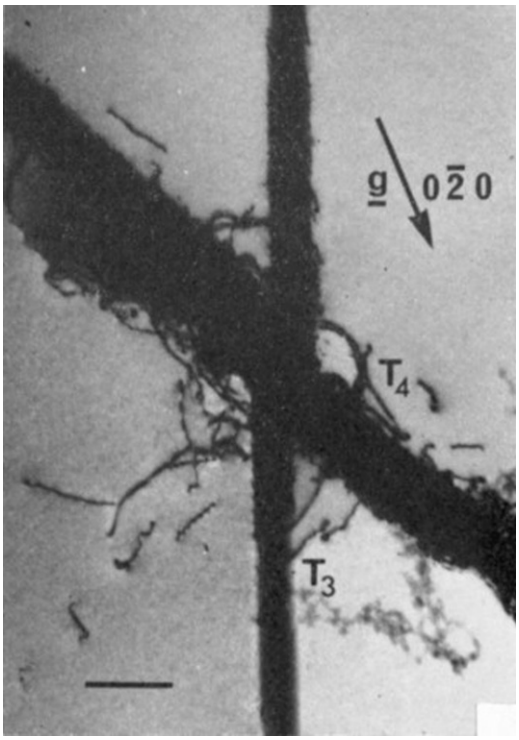

Figure 16 A ⟨012⟩ twin intersection observed in a deformed Mo–35 at% Re alloy sample (Mahajan, 1971).

a secondary twin has formed in the barrier twin (T_2) with a habit plane identified as $(1\bar{1}\bar{5}) = (\bar{1}11)_T$. The microstructure also contains some triangular-shaped striated regions, contiguous to the secondary twins, and some very small twins within T_1. The striated areas occur mainly on one, but occasionally on both sides of the secondary twins. These regions may also be subsidiary twins, but the way in which the complex structure has evolved is not known.

In polycrystalline materials, sub-boundaries are weak obstacles to twins, whereas general high-angle grain boundaries are strong barriers to twins. **Figure 18**, reproduced from the study of Mahajan (1973), shows how a twin interacts with a small-angle tilt boundary. The boundary is displaced as a result of the interaction. In addition, dislocation activity is observed on a slip plane that is defined by GG′ and HH′ and contains the line of intersection of the twin plane and the boundary. Dislocation activity was also observed in a grain across the boundary. Mahajan rationalized these observations by assuming the formation of emissary dislocations at the sub-boundary/twin intersection.

Figure 19 illustrates the complexities of a grain boundary–twin interaction (Mahajan, 1973). A number of events occur when a twin T_4 propagating in grain C interacts with a high-angle grain boundary. A slip band S_2 forms within grain C. The situation within grain D is much more complex. Three slip bands S_3, S_4, and S_5 evolve within Grain D. In addition, dislocation activity is observed along the boundary. Mahajan again explained these observations by assuming the formation of emissary dislocations at the boundary/twin intersection.

An interesting question is do twin–twin and grain boundary interactions have a role in the nucleation of fracture? There is contradiction between some of the published results on b.c.c. crystals. Some of the observations indicate that fracture could nucleate at twin–twin interactions, whereas other results show that this is not the case. This difference is probably a chemical effect since both fracture properties and twinning are sensitive to composition, but it may be linked to the relative growth rates of twins in different materials. Since the dislocation density cannot be increased instantaneously, the sudden imposition of a high strain rate in a localized region requires high dislocation velocities in order to accommodate the strain imposed by the twin by slip. In b.c.c. materials, where dislocation velocity is stress dependent, this in turn requires high local stresses, which may then exceed the stress required for crack nucleation. This suggests that cracks are more likely to form at twin intersections where crossing twins grow with high velocities into regions where the density of mobile dislocations is low.

4 Advanced Techniques for Studying Deformation Twinning in h.c.p. Materials

As reviewed in Sections 1–3, during the past 60 years, numerous experimental and theoretical studies have provided important fundamental insight into deformation twinning in f.c.c. and b.c.c. metals (Christian and Mahajan, 1995). However, it was not until the recent decade that twinning in h.c.p. materials has emerged as an important research topic of the research community. The

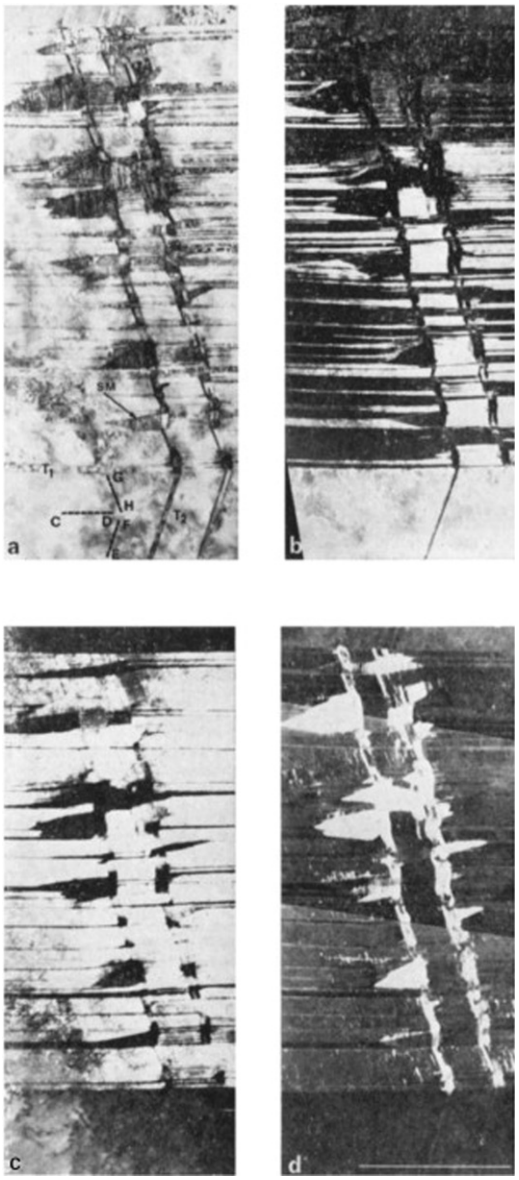

Figure 17 Twin interactions observed in a Co–8 wt% Fe alloy single crystal. The plane of the micrograph in each case is ~(110). Micrographs (b), (c), and (d) show dark-field images of the matrix, T_1, and secondary twins, respectively. The traces of $(\bar{1}1\bar{1})$, $(\bar{1}11)$, and $(1\bar{1}\bar{5})$ planes in the (110) plane are identified by CD, EF, and GH, respectively. SM refers to the twinned region in the matrix that may have undergone a shear reverse to that of T_2. The marker represents one micron (Mahajan and Chin, 1974).

reasons for this are many-fold: (1) there are multiple twinning modes in h.c.p. (see Section 1.3), whereas there is just one well-defined twinning mode in f.c.c. and b.c.c., (2) twinning dislocations in h.c.p. generally have very small Burgers vectors that are hardly visible in TEM, as opposed to larger Burgers vectors and visible twinning dislocations in f.c.c. and b.c.c., and (3) deformation twinning in h.c.p., especially the most common $\{10\bar{1}2\}$ twinning, nucleates readily and grows rapidly, which makes resolving the defect structure associated with twinning at different deformation stages a challenging task. Fortuitously, recent developments in advanced analytical techniques, such as EBSD and in-situ TEM, have facilitated in-depth and reliable characterization of twinning phenomena in h.c.p. materials, leading to new information on twinning mechanisms and related phenomena.

4.1 EBSD Research

Among the various twinning modes, the most common and profuse mode is $\{10\bar{1}2\}$ twinning, which re-orients the lattice by ~90° (Partridge, 1967; Christian and Mahajan, 1995). For example, in the case of single crystal deformation in Mg (Kelley and Hosford, 1968; Yu *et al.*, 2014), macroscopic $\{10\bar{1}2\}$ twins were readily nucleated and visible under compression along $[10\bar{1}0]$

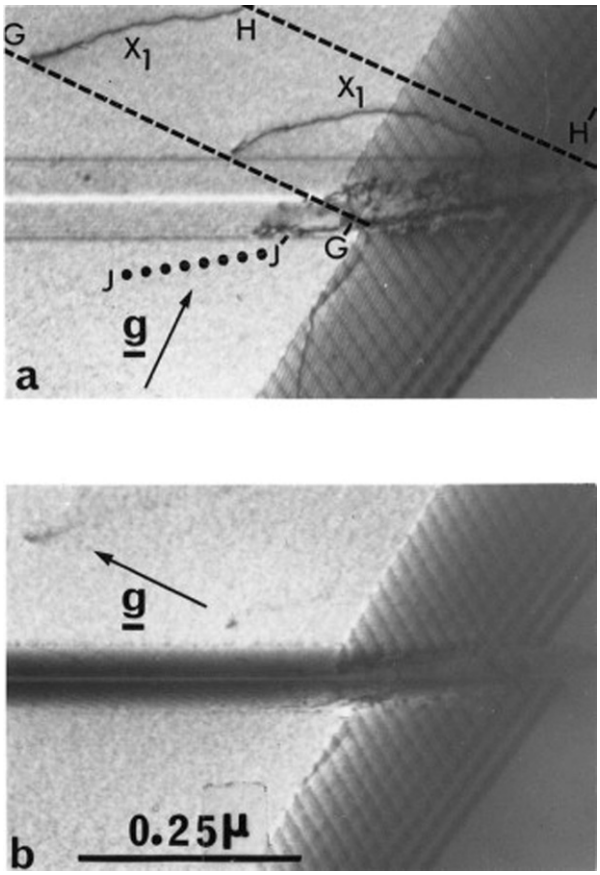

Figure 18 Micrographs showing the interaction of a twin with a sub-boundary in a deformed Mo–35 at% Fe alloy (Mahajan, 1973).

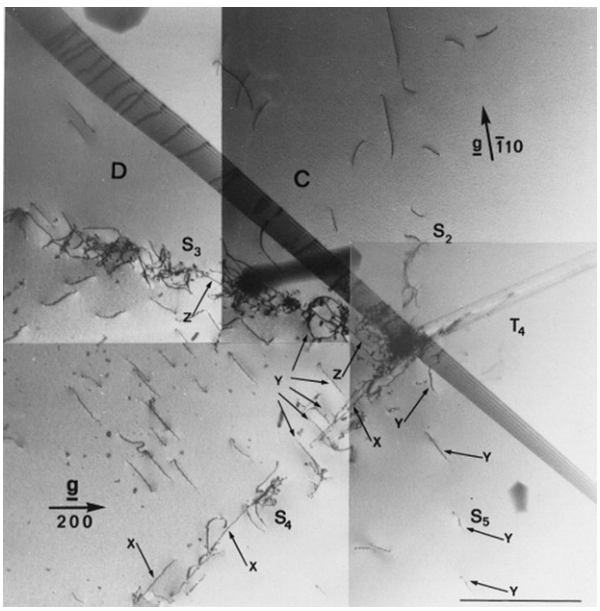

Figure 19 Micrograph showing substructure resulting from the interaction of a twin with a grain boundary in a deformed Mo–35 at% Fe alloy specimen (Mahajan, 1973).

direction with just 0.75% strain, or under tension along [0001] c-axis with just 0.5% strain. In related studies involving an extruded Mg alloy compressed along the extrusion direction (El Kadiri *et al.*, 2013), $\{10\bar{1}2\}$ twins propagated and 'consumed' most of grains at less than 8% strain. Therefore, the crystallographic re-orientation and morphological changes caused by twinning

in h.c.p. materials make EBSD a suitable and powerful tool for the study of twinning-related phenomena, e.g., twin nucleation, twin propagation/growth, twin–twin interactions, twin-grain boundary interactions (Beyerlein *et al.*, 2010). EBSD can provide not only abundant meso-scale information on crystallographic orientation and morphology for a statistically-relevant large area of interest (as large as several mm^2), but also provides local microscopic information on misorientation within each grain/twin, strain distribution, etc. These are advantages that conventional optical microscopy or TEM cannot provide.

Although it is difficult to characterize twin nucleation experimentally due to the fine atomic and nanometer scales involved, twin lamellae, on the other hand, are relatively easy to characterize using EBSD. It becomes readily apparent in any EBSD analysis of twinned microstructures that, unlike dislocation glide, the occurrence and physical characteristics of twin lamellae are statistical in nature, varying substantially across the microstructure. An automated imagine-analysis computer code developed by Marshall *et al.* (2010) was used to derive a suite of statistics on $\{10\bar{1}2\}$ tensile twins based on raw EBSD of deformed Zr and Mg (Capolungo *et al.*, 2009; Beyerlein *et al.*, 2010). The statistics included over thousands of twins and grains and produced correlations between $\{10\bar{1}2\}$ tensile twinning characteristics and grain characteristics. Important relations covered the presence of twins, number of twins, twin thickness, twin type, and twin variant with the orientation and size of the grain as well as those of its neighboring grains. It is found that twins are more likely to form and are thicker in grains that are well oriented for twinning. However, the twin variant formed is not necessarily the one possessing the highest Schmid factor. This discrepancy indicates that localized stress states, not sample averaged stress states, strongly influence the type and variant of the twin that forms.

These extensive experimental EBSD analyses show that twins in h.c.p. metals are frequently connected to grain boundaries (Capolungo *et al.*, 2009; Beyerlein *et al.*, 2010; Wang *et al.*, 2010a, 2010b). This consistent observation suggests that compared to the interior of the grains, and apart from any outstanding cracks or superficial defects, twins preferentially originate from grain boundaries. To date, there are very few in-situ observations of twin growth during deformation, although one recent observation using in-situ EBSD of an Mg–Ce alloy confirmed the notion that deformation twins form from grain boundaries (Adams *et al.*, 2011). Development of 'adjoining twin pairs' (ATPs) is another indication of grain boundary nucleation of deformation twins. An ATP configuration consists of two twins belonging to neighboring grains that meet at a common grain boundary at the same location. ATPs are often documented preferably at low angle grain boundaries (LAGBs), as shown in **Figure 20** (Zhang, 2015). The presence of ATPs suggests that twins may nucleate at both sides of LAGBs, as revealed by recent modeling work (Wang *et al.*, 2014).

In principle, the preferential formation of twins from grain boundaries may be anticipated. High stress states and large defects represent ideal conditions for activating deformation twins. Grain boundaries are arguably one of the more high-defect-density regions within a grain microstructure. They can contain misfit dislocations, ledges, stacking faults, and nano-voids, thus providing a variety of possible sources for forming twin embryos. In addition, grain boundaries tend to develop relatively high local stresses (Rollett *et al.*, 2010, Niezgoda *et al.*, 2014), which would be required to convert the defects within grain boundaries into twin embryos and eventually twin lamellae.

Due to the six-fold symmetry in the h.c.p. lattice, each twinning mode, including $\{10\bar{1}2\}$, $\{10\bar{1}1\}$, $\{10\bar{1}3\}$, $\{11\bar{2}2\}$, $\{11\bar{2}1\}$, and $\{11\bar{2}4\}$ (Yoo, 1981), has six crystallographic equivalent variants. Take $\{10\bar{1}2\}$ twin deformation twinning as an example. Since the $\{10\bar{1}2\}$ twin plane family has six actual planes: $(10\bar{1}2)$, $(1\bar{1}02)$, $(0\bar{1}12)$, $(\bar{1}012)$, $(\bar{1}102)$, and $(01\bar{1}2)$, correspondingly $\{10\bar{1}2\}$ twin has six variants, namely T1, T2, T3, T4, T5, T6, respectively.

Figure 21 (Zhang, 2015) shows some experimental results of $\{10\bar{1}2\}$ twin–twin interactions in a hot-rolled Mg plate compressed along the rolling direction (RD) by 3.8% strain at room temperature. The loading axis/RD is the horizontal direction in the figure. Therefore, the parent grain (namely the matrix) was deformed nearly perpendicular to its c-axis, and all the twins present are $\{10\bar{1}2\}$ twins with four different variants, namely T1, T3, T4, and T6. In **Figure 21(a)**, the color-coding is based on the different values of the three Euler angles for each scanned data point. In this way, each twin variant can be identified based on its color. For example, T1 and T3 (or T4 and T6) can simply be differentiated by color. Nevertheless, T1 and T4 (or T3 and T6) has nearly the same color, namely similar orientation – they are so-called "co-zone" twins, in that they share the same zone axis when twinning occurs, only one variant re-orient the lattice by $\sim 86^\circ$ in one direction (e.g., clockwise), while the other variant re-orient the lattice also by $\sim 86^\circ$ but in the opposite direction (e.g., counter-clockwise). Therefore, one needs to examine the shapes of each co-zone twins to further identify the twin plane in order to tell one from the other.

As the sample was deformed to a moderate strain (3.8%), more than half of the area examined was already consumed by twins, and different twin variants started to interact with each other in various ways. However, the twin–twin interactions can essentially be categorized into two types: co-zone interaction and non-co-zone interaction. As mentioned earlier, co-zone twins (e,g., T1 ~ T4 herein) exhibit similar orientation. Ideally, misorientation angle at the twin–twin boundary is $\sim 7.4^\circ$. However, due to possible slip transmission and macroscopic deformation, as well as the resolution limit of EBSD, the misorientation angle ranges between ~ 2 to $\sim 7^\circ$. In the case of non-co-zone interactions, such as T1–T3, T1–T6, T4–T3, T3–T6, the misorientation angle at a twin–twin boundary is $\sim 57^\circ$. This large angle is important to note as it means non-co-zone twin–twin interactions would create high angle boundaries within the original grain, thus dividing one grain into multiple grains and impeding slip. The blue and red arrowed lines are two examples showing the variation in misorientation angles across twin boundaries and/or twin–twin boundaries.

Moreover, based on detailed orientation information, EBSD also enables detailed Schmid factor calculation for various slip systems under different loading condition(s). **Figures 21(b)** and **21(c)** gives the Schmid factor 'map' in both twins and the matrix for

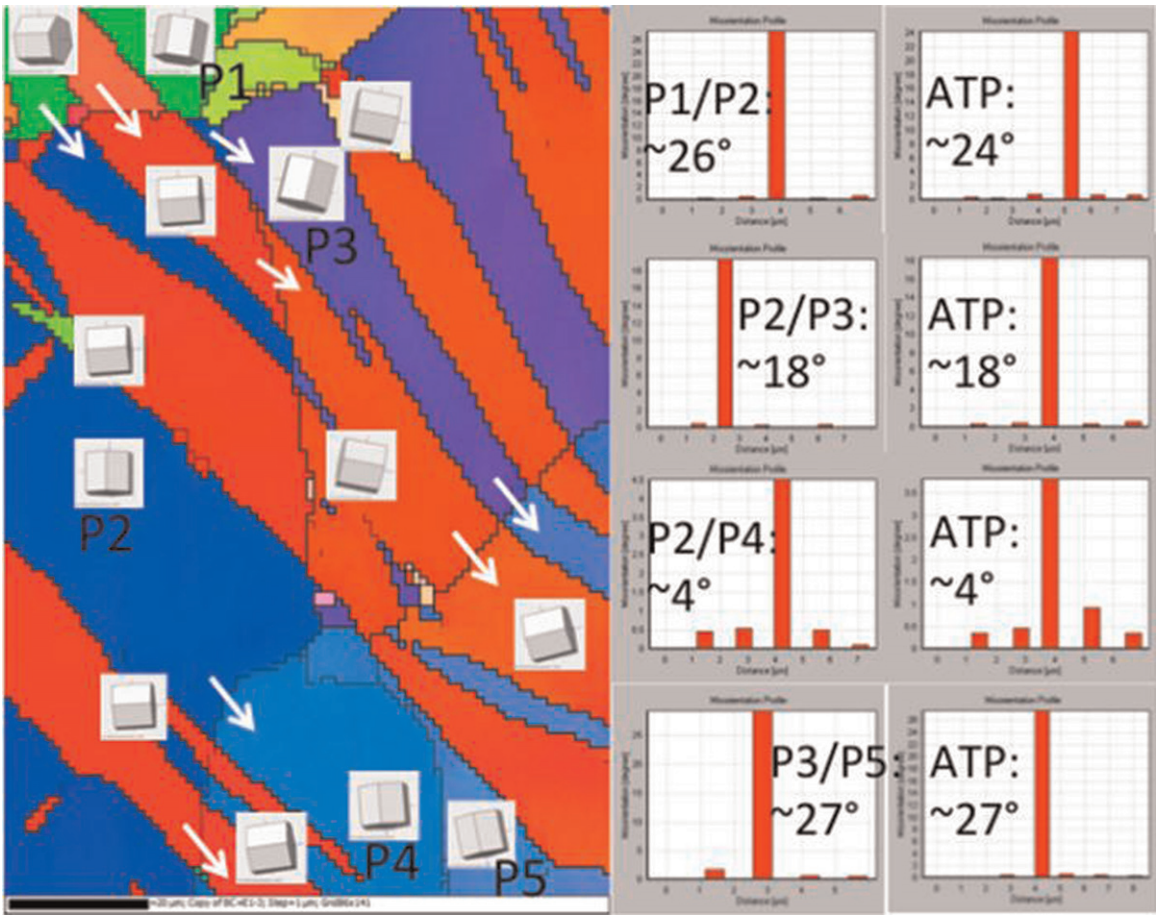

Figure 20 EBSD inverse pole figure colored map showing five neighboring grains (P1, P2, P3, P4, P5), their orientations, and misorientations across grain boundaries or adjoining twin pairs (Zhang, 2015).

basal slip and prismatic slip, respectively. It is noted that the original matrix is oriented favoring prismatic slip (red areas in (c)), yet twinning still dominated the observed deformation. Moreover, T1 twins (red areas in (b)) would favor basal slip during subsequent deformation. Therefore the dynamic interaction of twinning and slip can be provided by EBSD.

4.2 HRTEM and In-situ TEM studies

Twin domains, much like grains, can deform by slip and twinning. Formation of a separate twin domain within a pre-existing twin is called secondary twinning. Secondary twins are usually a different twin variant or twin type than the parent twin. Secondary twinning has been observed in Mg, Zr, Ti, and their alloys (Wonsiewicz and Backofen, 1967; Barnett, 2007; Bozzolo *et al.*, 2010; Proust *et al.*, 2010). In Mg, a commonly observed primary-secondary twin pair is the so called $\{10\bar{1}1\}$–$\{10\bar{1}2\}$ double twin, which is created when a $\{10\bar{1}2\}$ extension twin forms within the domain of a contraction $\{10\bar{1}1\}$ twin. Double twins have been studied in Mg (Wonsiewicz and Backofen, 1967) and Mg alloys, like AZ31 (Barnett; 2007; Barnett *et al.*, 2008; Cizek and Barnett, 2008; Mu *et al.*, 2012; Ando *et al.*, 2014), ZK60 (Barnett, 2007), L4 (Lentz *et al.*, 2014) and LA41 (Lentz *et al.*, 2014). Unlike {10–12} twins, which grow to thicknesses on the order of the grain diameter, contraction $\{10\bar{1}1\}$ twins and double twins are often observed to be very fine and needle-like.

Double twins are thought to form as a result of basal ⟨a⟩ slip within the domain of the $\{10\bar{1}1\}$ compression twin. The same stress state that can activate a primary $\{10\bar{1}1\}$ compression twin is not suitable for activating basal <a> slip within the grain. However, within the $\{10\bar{1}1\}$ twin lamella, the *c*-axis has been reoriented by 56°, making the twin domain, unlike the parent grain, favorable for basal ⟨a⟩ slip. Detailed TEM and HRTEM investigations have provided evidence of profuse basal slip confined within the $\{10\bar{1}1\}$ twins but not the parent (Lentz *et al.*, 2014). When gliding basal slip dislocations within the twin interact with the $\{10\bar{1}1\}$ twin boundary, they can dissociate into $\{10\bar{1}2\}$ twinning dislocations (Beyerlein *et al.*, 2012). An internal $\{10\bar{1}2\}$ twin can form when a sufficient number of dissociation reactions take place to produce enough twinning dislocations to transform into a stable $\{10\bar{1}2\}$ twin embryo (see Section 1.3 on twin nucleation).

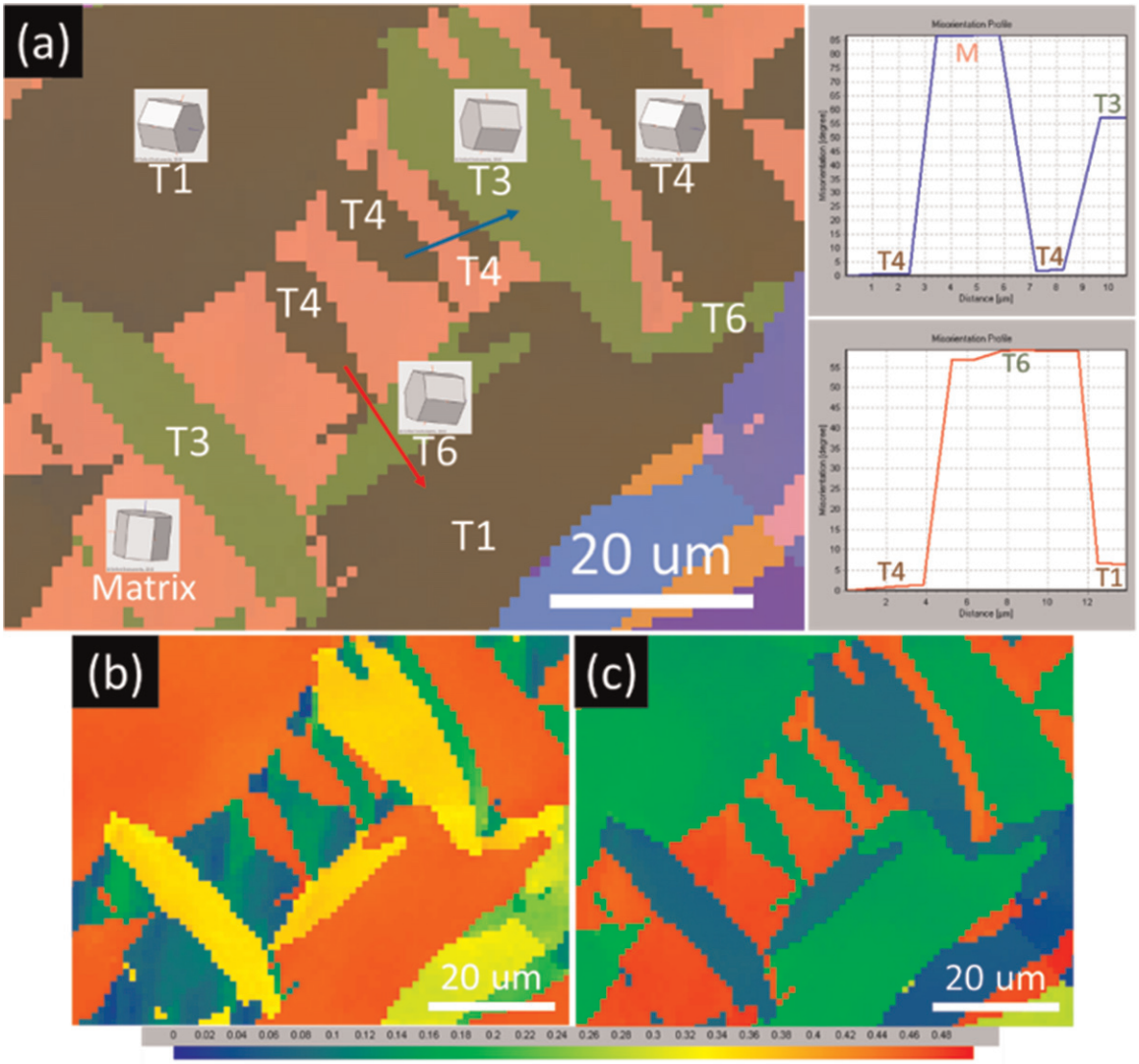

Figure 21 (a). Twin–twin interactions and misorientation angles across twin boundaries and twin–twin boundaries. EBSD Euler angle map acquired from a hot-rolled Mg plate deformed to 3.8% strain. Each hexagonal prism represents the orientation of corresponding twin variant. (b) and (c), Schmid factor maps for basal and prism slip, respectively. The rainbow color bar indicates Schmid factor values (Zhang, 2015).

The formation of $\{10\bar{1}1\}$–$\{10\bar{1}2\}$ double twins has been linked to fracture processes. The double twin domain is well oriented for basal ⟨a⟩ slip. At present, it is believed that the high concentration of basal ⟨a⟩ slip within the fine needle-like domain of the double twins will promote strain localization, fracture, and void formation (Wonsiewicz and Backofen, 1967; Barnett *et al.*, 2008; Ando *et al.*, 2014).

In addition to EBSD, in-situ TEM deformation has been used to dynamically capture the nucleation and growth of deformation twinning in h.c.p. materials. In related studies, Yu *et al.* (Qian and Mishra, 2012; Somekawa and Schuh, 2012; Yu *et al.*, 2012) performed in-situ TEM tension tests on single-crystal h.c.p. Mg pillars oriented along [0001]. Instead of a single twin, they observed the formation of many $\{10\bar{1}2\}$ nano-twins across the entire sample length (**Figures 22(a)–22(c)**). Liu *et al.* (2014) conducted in-situ TEM compression along the prismatic plane of submicron single-crystal Mg pillars (**Figures 22(d)–22(j)**). Interestingly, they demonstrated deformation twinning with an orientation relationship akin to that of the conventional $\{10\bar{1}2\}$ twinning, but without a crystallographic mirror plane. The boundary was revealed to be composed predominantly of semi-coherent basal/prismatic interfaces instead of the $\{10\bar{1}2\}$ twinning plane (**Figures 22(h)–22(j)**). Most surprisingly, they found that the 'twin' boundary mediated by basal/prismatic interfaces can propagate without an obvious twinning shear (**Figure 22(f)**), which can be explained by the $\{10\bar{1}2\}$ twin nucleation mechanisms discussed in Section 1.3.

In addition, in-situ TEM deformation techniques have provided new insights into the correlation of deformation twinning and mechanical behavior. Yu *et al.* (Yu *et al.*, 2010; Qian and Mishra, 2012; Somekawa and Schuh, 2012; Yu *et al.*, 2012) has demonstrated strong sample size effects on the deformation twinning in h.c.p. Mg and Ti, in which the nucleation stress required

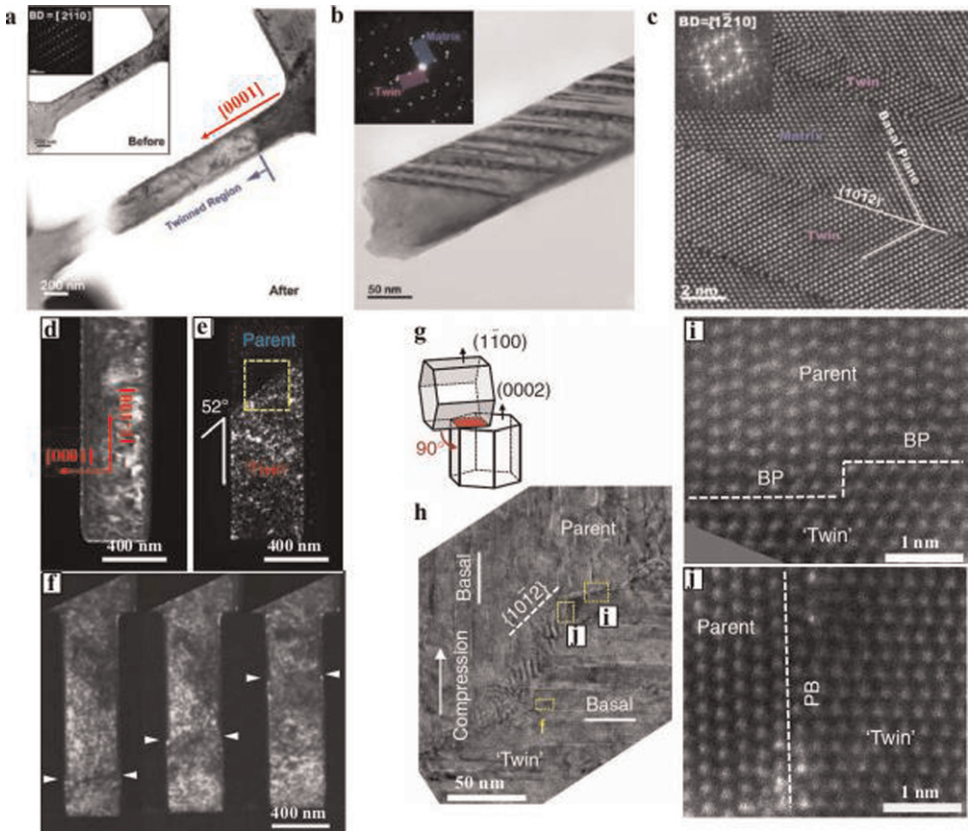

Figure 22 TEM images from in-situ tensile tests of [0001] oriented Mg pillars (Qian and Mishra, 2012; Somekawa and Schuh, 2012; Yu *et al.*, 2012): (a) Fracture occurred at the end of the twinned region. The inset is an image of the sample before the test. The loading axis is normal to the basal plane of the crystal. (b) Nano-twin array in a tensile sample. (c) A typical high-resolution TEM (HRTEM) image of the nano-twins from a near surface region where the finest twins were found. (d and e) Dark-field TEM images showing the pillar before and after loading, respectively. (f) Snapshots extracted from the recorded movie showing that basal/prismatic interfaces mediated twin boundary migration (marked by a pair of white arrows) with time. (g) Schematic showing the orientation relationship between the twin and its parent lattice; (h) HRTEM image showing the rugged twin boundary (see atomic resolution images in i and j), with stacking faults on both sides of the boundary. (i, j) Scanning TEM images of typical basal/prismatic (BP) interface and prismatic/basal (PB) interface, respectively (Liu *et al.*, 2014).

for deformation twinning increases drastically with decreasing pillar size of a Ti or Mg alloy single crystal, until the pillar size is reduced to one micrometer, below which the deformation twinning is entirely replaced by dislocation plasticity. The critical stress for $\{10\bar{1}1\}$ compression twin nucleation in pure Mg submicron pillars was found to approach 750 MPa (Yu *et al.*, 2012). Whereas the critical resolved shear stress for $\{10\bar{1}2\}$ and $\{10\bar{1}1\}$ deformation twinning in bulk Mg samples, were reported to be $\sim$3 and $\sim$100 MPa, respectively (Yu *et al.*, 2012). Work hardening contributed by deformation twinning has also been well demonstrated by the in-situ TEM deformation. In Yu *et al.*'s work (Yu *et al.*, 2012), significant strain hardening was obtained after the formation of a nano-twinned structure in single crystal Mg pillars, presumably resulting from the high density of twin boundaries, which serve as barriers to further dislocation motion.

In summary, dislocation mechanisms for the formation of twins in b.c.c., f.c.c., and h.c.p. crystals have been briefly reviewed. An attempt has been made to understand in terms of these models the influence of temperature, composition, pre-strain, and microstructure on deformation twinning. Furthermore, accommodation processes occurring at twins terminating within a crystal, and twin–twin and grain boundary interactions are covered. Finally, recent advances in understanding twinning in h.c.p. materials using EBSD and HRTEM/in-situ TEM are briefly reviewed.

Acknowledgments

This work was supported by National Science Foundation (NSF CMMI-1437327).

References

Adams, B.L., Fullwood, D.T., Basinger, J., Hardin, T., 2011. High resolution EBSD-based dislocation microscopy. Materials Science Forum 702–703, 11–17.

Agnew, S.R., Tomé, C.N., Brown, D.W., Holden, T.M., Vogel, S.C., 2003. Study of slip mechanisms in a magnesium alloy by neutron diffraction and modeling. Scripta Materialia 48 (8), 1003–1008.
Ando, D., Koike, J., Sutou, Y., 2014. The role of deformation twinning in the fracture behavior and mechanism of basal textured magnesium alloys. Materials Science and Engineering: A 600, 145–152.
Armstrong, R., Codd, I., Douthwaite, R.M., Petch, N.J., 1962. The plastic deformation of polycrystalline aggregates. Philosophical Magazine 7 (73), 45–58.
Barnett, M.R., 2007. Twinning and the ductility of magnesium alloys: Part II. "Contraction" twins. Materials Science and Engineering: A 464 (1–2), 8–16.
Barnett, M.R., 2008. A rationale for the strong dependence of mechanical twinning on grain size. Scripta Materialia 59 (7), 696–698.
Barnett, M.R., Keshavarz, Z., Beer, A.G., Atwell, D., 2004. Influence of grain size on the compressive deformation of wrought Mg–3Al–1Zn. Acta Materialia 52 (17), 5093–5103.
Barnett, M.R., Keshavarz, Z., Beer, A.G., Ma, X., 2008. Non-Schmid behaviour during secondary twinning in a polycrystalline magnesium alloy. Acta Materialia 56 (1), 5–15.
Beyerlein, I.J., Capolungo, L., Marshall, P.E., McCabe, R.J., Tome, C.N., 2010. Statistical analyses of deformation twinning in magnesium. Philosophical Magazine 90 (16), 2161–2190.
Beyerlein, I.J., McCabe, R.J., Tomé, C.N., 2011. Effect of microstructure on the nucleation of deformation twins in polycrystalline high-purity magnesium: A multi-scale modeling study. Journal of the Mechanics and Physics of Solids 59 (5), 988–1003.
Beyerlein, I.J., Tome, C.N., 2010. A probabilistic twin nucleation model for HCP polycrystalline metals. Proceedings of the Royal Society A – Mathematical Physical and Engineering Sciences 466 (2121), 2517–2544.
Beyerlein, I.J., Wang, J., Barnett, M.R., Tome, C.N., 2012. Double twinning mechanisms in magnesium alloys via dissociation of lattice dislocations. Proceedings of the Royal Society A – Mathematical Physical and Engineering Sciences 468 (2141), 1496–1520.
Bozzolo, N., Chan, L., Rollett, A.D., 2010. Misorientations induced by deformation twinning in titanium. Journal of Applied Crystallography 43 (3), 596–602.
Brown, D.W., Almer, J.D., Clausen, B., *et al.*, 2013. Twinning and de-twinning in beryllium during strain path changes. Materials Science and Engineering: A 559, 29–39.
Capolungo, L., Marshall, P.E., McCabe, R.J., Beyerlein, I.J., Tomé, C.N., 2009. Nucleation and growth of twins in Zr: A statistical study. Acta Materialia 57 (20), 6047–6056.
Cerreta, E., Mahajan, S., 2001. Formation of deformation twins in TiAl. Acta Materialia 49 (18), 3803–3809.
Chin, G., Hosford, W., Mendorf, D., 1969. Accommodation of constrained deformation in fcc metals by slip and twinning. Proceedings of the Royal Society of London A: Mathematical, Physical and Engineering Sciences.
Christian, J.W., Mahajan, S., 1995. Deformation twinning. Progress in Materials Science 39 (1–2), 1–157.
Cizek, P., Barnett, M.R., 2008. Characteristics of the contraction twins formed close to the fracture surface in Mg–3Al–1Zn alloy deformed in tension. Scripta Materialia 59 (9), 959–962.
Cottrell, A.H., Bilby, B.A., 1951. LX. A mechanism for the growth of deformation twins in crystals. The London, Edinburgh, and Dublin Philosophical Magazine and Journal of Science 42 (329), 573–581.
Dubertret, A., Le Lann, A., 1980. Development of a new model for atom movement in twinning. Case of the {1011}, {1013} twins and {1011} {1012} double twinning in H.C.P. metals. Physica Status Solidi (a) 60 (1), 145–151.
El Kadiri, H., Kapil, J., Oppedal, A.L., *et al.*, 2013. The effect of twin–twin interactions on the nucleation and propagation of twinning in magnesium. Acta Materialia 61 (10), 3549–3563.
Gray III, G.T., 1988. Deformation twinning in Al–4.8 wt% Mg. Acta Metallurgica 36 (7), 1745–1754.
Hull, D., 1963. Growth of twins and associated dislocation phenomena. In: Reed-Hill, R.E., Hirth, J.P., Rogers, H.C. (Eds.), Deformation Twinning. New York: Gordon and Breach, pp. 121–155.
Kelley, E.W., Hosford, W.F., 1968. Plane-strain compression of magnesium and magnesium alloy crystals. Transactions of the Metallurgical Society of AIME 242 (1), 5–6.
Knezevic, M., Zecevic, M., Beyerlein, I.J., Bingert, J.F., McCabe, R.J., 2015. Strain rate and temperature effects on the selection of primary and secondary slip and twinning systems in HCP Zr. Acta Materialia 88 (0), 55–73.
Lann, A.L., Dubertret, A., 1979. A development of Kronberg's model for {1012} twins in H.C.P. metals. Extension to {1122} twins. Physica Status Solidi (a) 51 (2), 497–507.
Lentz, M., Behringer, A., Fahrenson, C., Beyerlein, I., Reimers, W., 2014. Grain size effects on primary, secondary, and tertiary twin development in Mg–4 wt pct Li (– 1 wt pct Al) alloys. Metallurgical and Materials Transactions A 45 (11), 4737–4741.
Lentz, M., Coelho, R.S., Camin, B., *et al.*, 2014. In-situ, ex-situ EBSD and (HR-)TEM analyses of primary, secondary and tertiary twin development in an Mg–4 wt%Li alloy. Materials Science and Engineering: A 610 (0), 54–64.
Li, B., Ma, E., 2009. Atomic shuffling dominated mechanism for deformation twinning in magnesium. Physical Review Letters 103 (3), 035503.
Liu, B.Y., Wang, J., Li, B., *et al.*, 2014. Twinning-like lattice reorientation without a crystallographic twinning plane. Nature Communications 5, 3297.
Lou, X.Y., Li, M., Boger, R.K., Agnew, S.R., Wagoner, R.H., 2007. Hardening evolution of AZ31B Mg sheet. International Journal of Plasticity 23 (1), 44–86.
Mahajan, S., 1971. Twin-slip and twin-twin interactions in Mo–35 at% Re alloy. Philosophical Magazine 23 (184), 781–794.
Mahajan, S., 1972a. Evaluation of slip patterns observed in association with deformation twins in Mo–35 at percent Re alloy. Journal of Physics F – Metal Physics 2 (1), 19–20.
Mahajan, S., 1972b. Nucleation and growth of deformation twins in Mo–35 at% Re alloy. Philosophical Magazine 26 (1), 161–171.
Mahajan, S., 1973. Observations on interaction of twins with grain-boundaries in Mo–35 at percent re alloy. Acta Metallurgica 21 (3), 255–260.
Mahajan, S., 1975a. The evolution of intrinsic–extrinsic faulting in fcc crystals. Metallurgical Transactions A 6 (10), 1877–1886.
Mahajan, S., 1975b. Interrelationship between slip and twinning in BCC crystals. Acta Metallurgica 23 (6), 671–684.
Mahajan, S., 2013. Critique of mechanisms of formation of deformation, annealing and growth twins: Face-centered cubic metals and alloys. Scripta Materialia 68 (2), 95–99.
Mahajan, S., Chin, G.Y., 1973a. Formation of deformation twins In fcc crystals. Acta Metallurgica 21 (10), 1353–1363.
Mahajan, S., Chin, G.Y., 1973b. Twin–slip, twin–twin and slip–twin interactions in Co–8 wt percent Fe alloy single-crystals. Acta Metallurgica 21 (2), 173–179.
Mahajan, S., Chin, G.Y., 1974. Interaction of twins with existing substructure and twins in cobalt-iron alloys. Acta Metallurgica 22 (9), 1113–1119.
Mahajan, S., Jin, S., Brasen, D., 1980. Micro-twinning in a spinodally decomposed Fe–Cr–Co alloy. Acta Metallurgica 28 (7), 971–977.
Marshall, P.E., Proust, G., Rogers, J.T., McCabe, R.J., 2010. Automatic twin statistics from electron backscattered diffraction data. Journal of Microscopy 238 (3), 218–229.
Mu, S., Jonas, J.J., Gottstein, G., 2012. Variant selection of primary, secondary and tertiary twins in a deformed Mg alloy. Acta Materialia 60 (5), 2043–2053.
Niezgoda, S.R., Kanjarla, A.K., Beyerlein, I.J., Tomé, C.N., 2014. Stochastic modeling of twin nucleation in polycrystals: An application in hexagonal close-packed metals. International Journal of Plasticity 56 (0), 119–138.
Okazaki, K., Conrad, H., 1973. Effects of interstitial content and grain size on the strength of titanium at low temperatures. Acta Metallurgica 21 (8), 1117–1129.
Partridge, P.G., 1967. The crystallography and deformation modes of hexagonal close-packed metals. International Materials Reviews 12 (1), 169–194.
Proust, G., Kaschner, G.C., Beyerlein, I.J., *et al.*, 2010. Detwinning of high-purity zirconium: In-situ neutron diffraction experiments. Experimental Mechanics 50 (1), 125–133.
Proust, G., Tomé, C.N., Jain, A., Agnew, S.R., 2009. Modeling the effect of twinning and detwinning during strain-path changes of magnesium alloy AZ31. International Journal of Plasticity 25 (5), 861–880.
Qian, Y., Mishra, R.K., Minor, A.M., 2012. The effect of size on the deformation twinning behavior in hexagonal close-packed Ti and Mg. Jom 64 (10), 1235–1240.
Robertson, I.M., 1986. Microtwin formation in deformed nickel. Philosophical Magazine A 54 (6), 821–835.
Rollett, A.D., Lebensohn, R.A., Groeber, M., *et al.*, 2010. Stress hot spots in viscoplastic deformation of polycrystals. Modelling and Simulation in Materials Science and Engineering 18 (7),

Serra, A., Bacon, D.J., . A new model for {10(1)over-bar2} twin growth in hcp metals. Philosophical Magazine A – Physics of Condensed Matter Structure Defects and Mechanical Properties 73, 333–343.
Serra, A., Pond, R.C., Bacon, D.J., 1991. Computer simulation of the structure and mobility of twinning disclocations in H.C.P. metals. Acta Metallurgica et Materialia 39 (7), 1469–1480.
Sleeswyk, A.W., 1962. Emissary dislocations: Theory and experiments on the propagation of deformation twins in α-iron. Acta Metallurgica 10 (8), 705–725.
Sleeswyk, A.W., 1963. ½⟨111⟩ Screw dislocations and the nucleation of {112}⟨111⟩ twins in the b.c.c. lattice. Philosophical Magazine 8 (93), 1467–1486.
Somekawa, H., Schuh, C.A., 2012. High-strain-rate nanoindentation behavior of fine-grained magnesium alloys. Journal of Materials Research 27 (09), 1295–1302.
Song, S.G., Gray III, G.T., 1995a. Structural interpretation of the nucleation and growth of deformation twins in Zr and Ti – I. Application of the coincidence site lattice (CSL) theory to twinning problems in h.c.p. structures. Acta Metallurgica et Materialia 43 (6), 2325–2337.
Song, S.G., Gray III, G.T., 1995b. Structural interpretation of the nucleation and growth of deformation twins in Zr and Ti – II. TEM study of twin morphology and defect reactions during twinning. Acta Metallurgica et Materialia 43 (6), 2339–2350.
Suzuki, H., Barrett, C.S., 1958. Deformation twinning in silver-gold alloys. Acta Metallurgica 6 (3), 156–165.
Thompson, N., Millard, D.J., 1952. XXXVIII. Twin formation, in cadmium. The London, Edinburgh, and Dublin Philosophical Magazine and Journal of Science 43 (339), 422–440.
Vaidya, S., Mahajan, S., 1980. Accommodation and formation of (1121) twins in co single-crystals. Acta Metallurgica 28 (8), 1123–1131.
Venables, J.A., 1961. Deformation twinning in face-centred cubic metals. Philosophical Magazine 6 (63), 379–396.
Wang, J., Beyerlein, I.J., Hirth, J.P., 2012. Nucleation of elementary {(1)over-bar 0 1 1} and {(1)over-bar 0 1 3} twinning dislocations at a twin boundary in hexagonal close-packed crystals. Modelling and Simulation in Materials Science and Engineering 20 (2), 024001.
Wang, J., Beyerlein, I.J., Tomé, C.N., 2014. Reactions of lattice dislocations with grain boundaries in Mg: Implications on the micro scale from atomic-scale calculations. International Journal of Plasticity 56, 156–172.
Wang, J., Hirth, J.P., Tomé, C.N., 2009a. (– 1012) Twinning nucleation mechanisms in hexagonal-close-packed crystals. Acta Materialia 57 (18), 5521–5530.
Wang, J., Hoagland, R.G., Hirth, J.P., *et al.*, 2009b. Nucleation of a twin in hexagonal close-packed crystals. Scripta Materialia 61 (9), 903–906.
Wang, J., Yadav, S.K., Hirth, J.P., Tomé, C.N., Beyerlein, I.J., 2013. Pure-shuffle nucleation of deformation twins in hexagonal-close-packed metals. Materials Research Letters 1 (3), 126–132.
Wang, L., Eisenlohr, P., Yang, Y., Bieler, T.R., Crimp, M.A., 2010a. Nucleation of paired twins at grain boundaries in titanium. Scripta Materialia 63 (8), 827–830.
Wang, L., Yang, Y., Eisenlohr, P., *et al.*, 2010b. Twin nucleation by slip transfer across grain boundaries in commercial purity titanium. Metallurgical and Materials Transactions A 41 (2), 421–430.
Wonsiewicz, B.C., Backofen, W.A., 1967. Plasticity of magnesium crystals. Transactions of the Metallurgical Society of AIME 239 (9), 1422–1423.
Wu, X., Kalidindi, S.R., Necker, C., Salem, A.A., 2007. Prediction of crystallographic texture evolution and anisotropic stress–strain curves during large plastic strains in high purity α-titanium using a Taylor-type crystal plasticity model. Acta Materialia 55 (2), 423–432.
Xu, B., Capolungo, L., Rodney, D., 2013. On the importance of prismatic/basal interfaces in the growth of twins in hexagonal close packed crystals. Scripta Materialia 68 (11), 901–904.
Yoo, M.H., 1981. Slip, twinning, and fracture in hexagonal close-packed metals. Metallurgical Transactions A – Physical Metallurgy and Materials Science 12 (3), 409–418.
Yoo, M.H., 1997. On the dislocation pole mechanism for twinning in TiAl crystals. Philosophical Magazine Letters 76 (4), 259–268.
Yu, Q., Qi, L., Chen, K., *et al.*, 2012. The nanostructured origin of deformation twinning. Nano Letters 12 (2), 887–892.
Yu, Q., Shan, Z.W., Li, J., *et al.*, 2010. Strong crystal size effect on deformation twinning. Nature 463 (7279), 335–338.
Yu, Q., Wang, J., Jiang, Y., *et al.*, 2014. Twin–twin interactions in magnesium. Acta Materialia 77 (0), 28–42.
Zhang, D., *et al.*, 2015. in preparation.
Zhu, Y.T., Liao, X.Z., Wu, X.L., 2012. Deformation twinning in nanocrystalline materials. Progress in Materials Science 57 (1), 1–62.